Non-overlapping Schwarz algorithm for solving 2D m-DDFV schemes

FRANCK BOYER
Université Paul Cézanne, Laboratoire d'Analyse, Topologie et Probabilités
FST Saint-Jérôme, Case Cour A
Avenue escadrille Normandie-Niemen, 13397 Marseille Cedex 20, France

FLORENCE HUBERT & STELLA KRELL
Université de Provence, Laboratoire d'Analyse, Topologie et Probabilités,
39 rue F. Joliot-Curie, 13453 Marseille Cedex 13, France

We propose a non-overlapping Schwarz algorithm for solving "Discrete Duality Finite Volume" schemes (DDFV for short) on general meshes. In order to handle this problem, the first step is to propose and study a convenient DDFV scheme for anisotropic elliptic problems with mixed Dirichlet/Fourier boundary conditions. Then, we are able to build the corresponding Schwarz algorithm and to prove its convergence to the solution of the DDFV scheme on the initial domain. We finally give some numerical results both in the case where the Schwarz iterations are used as a solver or as a preconditioner.

Keywords: Finite volume methods, Schwarz Algorithm, DDFV methods.

1. Introduction

We are interested in this paper in finite volume numerical methods for solving second order linear elliptic problems in a domain Ω. In particular, we study discrete non-overlapping Schwarz methods in order to solve such scheme, taking advantage of a decomposition of Ω into subdomains.

The classical Schwarz iterative method, first devised at a theoretical level to treat complex domains, only converges when there is overlap between the subdomains. Furthermore, its convergence is very slow for small overlap sizes. In order to obtain convergent non-overlapping variants, different transmission conditions on the interfaces between the subdomains have been investigated. The first such non-overlapping method is based on Fourier transmission conditions. At the continuous level, this algorithm was first introduced and studied by Lions for Laplace operators in [13]. It has been adapted to several discrete approximation of isotropic diffusion problems (see [1], [4] and [9]). This paper is devoted to the development of a discrete counterpart of this non-overlapping Schwarz iterative method, with Fourier interface conditions, in the context of the DDFV schemes for general linear elliptic problems. The adaptation of this method to the discrete framework is very useful since each subdomain of a non-overlapping decomposition of the domain Ω can be meshed independently.

We do not consider here the problem of finding optimized non-overlapping methods as it has been done for instance in [7], [8] by introducing generalized transmission conditions. We only give numerical experiments (see section 5.5) illustrating the influence of the choice of the Fourier parameter on the overall performances of the algorithm. In particular, we observe a quite poor performance of the method even for the optimal choice of the parameter, that is to say that a large number of iterations are necessary to achieve a given precision. Nevertheless, it is well known (see for instance [14]) that such non optimized methods can be seen as a particular block Jacobi iterative solver and can be efficiently used as a preconditioner for any other iterative solver (GMRES, conjugate gradient, ...). We study in section 5.6 the performances of the conjugate gradient method preconditioned with our discrete non overlapping Schwarz algorithm for solving the DDFV finite volume scheme on the whole domain Ω.

The DDFV method has been developed to approximate anisotropic diffusion problems on general meshes. More precisely, it has been first introduced and studied in [6, 12] to approximate the Laplace equation with Dirichlet boundary conditions or homogeneous Neumann boundary conditions on a large class of 2D meshes including non-conformal and distorted meshes. Such schemes require unknowns on both vertices and centers of primal control volumes and allow us to build two-dimensional discrete gradient and divergence operators being in duality in a discrete sense. The DDFV scheme is extended in [2] to the case of the approximation of solutions to general linear and nonlinear elliptic problems with non homogeneous Dirichlet boundary conditions, including the case of anisotropic elliptic problems.

Convergence of such schemes is shown in [2] and *a priori* error estimates are given in the case where the coefficients of the operator and the exact solution u are assumed to be smooth enough. In [3], a modified DDFV scheme, called m-DDFV, is proposed and analysed in order to take into account possible discontinuities in the coefficients of the elliptic problem under study. In particular, first order convergence of the m-DDFV scheme is proved for the problem (1.1) with $\Gamma = \emptyset$ and piecewise smooth coefficients. This framework is recalled in Section 2.

In Section 3, we propose to adapt the m-DDFV scheme to mixed Dirichlet/Fourier boundary conditions :

$$\begin{cases} -\text{div}(A(x)\nabla u(x)) = f(x), & \text{in } \Omega, \\ u = h, & \text{on } \partial\Omega \setminus \Gamma, \\ -(A\nabla u, \vec{n}) = \lambda u - g, & \text{on } \Gamma. \end{cases} \tag{1.1}$$

where Ω is an open bounded polygonal domain of $\mathbb{R}^2$. The measurable matrix-valued map $A : \Omega \to \mathcal{M}_{2,2}(\mathbb{R})$ is supposed to fulfill the following assumption: there exists $C_A > 0$ such that

$$(A(x)\xi, \xi) \geqslant \frac{1}{C_A}|\xi|^2, \text{ and } |A(x)\xi| \leqslant C_A|\xi|, \ \forall \xi \in \mathbb{R}^2, \text{ and for a.e. } x \in \Omega.$$

This assumption ensures that the Problem (1.1) has a unique solution in $H^1(\Omega)$ for any $f \in H^{-1}(\Omega)$ and $h,\ g \in H^{\frac{1}{2}}(\partial\Omega)$. We restrict our attention, in this paper, to source terms $f \in L^2(\Omega)$. The parameter $\lambda > 0$ is given and Γ is an open subset of $\partial\Omega$.

With these preliminary results at hand we describe in Section 4 the non-overlapping iterative method we propose and prove its convergence.

We finally give in Section 5 some numerical results illustrating the performance of the iterative Schwarz algorithm.

2. The DDFV framework

The meshes: we recall here the main notations and definitions taken from [2]. A DDFV mesh $\mathcal{T}$ is constituted by a primal mesh $\mathfrak{M}$ and a dual mesh $\mathfrak{M}^* \cup \partial\mathfrak{M}^*$ (Figure 2.1).

The primal mesh $\mathfrak{M}$ is a set of disjoint open polygonal control volumes $\kappa \subset \Omega$ such that $\cup\overline{\kappa} = \overline{\Omega}$. We denote by $\partial\mathfrak{M}$ the set of edges of the control volumes in $\mathfrak{M}$ included in $\partial\Omega$, which we consider as degenerate control volumes. To each control volume and degenerate control volume $\kappa \in \mathfrak{M} \cup \partial\mathfrak{M}$, we associate a point $x_\kappa \in \kappa$. This family of points is denoted by $X = \{x_\kappa,\ \kappa \in \mathfrak{M} \cup \partial\mathfrak{M}\}$.

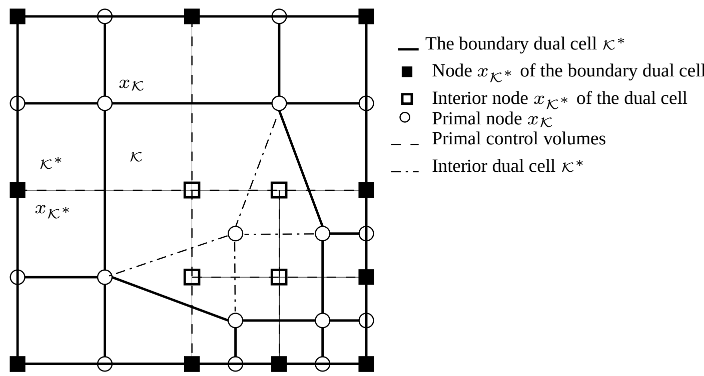

FIG. 2.1. The mesh $\mathcal{T}$

Let X^* denote the set of the vertices of the primal control volumes in $\mathfrak{M}$ that we split into $X^* = X^*_{int} \cup X^*_{ext}$ where $X^*_{int} \cap \partial\Omega = \emptyset$ and $X^*_{ext} \subset \partial\Omega$. With any point $x_{\mathcal{K}^*} \in X^*_{int}$ (resp. $x_{\mathcal{K}^*} \in X^*_{ext}$), we associate the polygon $\mathcal{K}^*$ whose vertices are $\{x_{\mathcal{K}} \in X, \text{ such that } x_{\mathcal{K}^*} \in \overline{\mathcal{K}},\ \mathcal{K} \in \mathfrak{M}\}$ (resp. $\{x_{\mathcal{K}^*}\} \cup \{x_{\mathcal{K}} \in X, \text{ such that } x_{\mathcal{K}^*} \in \overline{\mathcal{K}},\ \mathcal{K} \in (\mathfrak{M} \cup \partial\mathfrak{M})\}$) sorted with respect to the clockwise order of the corresponding control volumes. This defines the set $\mathfrak{M}^* \cup \partial\mathfrak{M}^*$ of dual control volumes.

REMARK 2.1 *Remark that our dual control volumes are not exactly the same than in [5] or [12]. In [5], $\mathcal{K}^*$ is a union of triangles $[x_{\mathcal{K}}, x_\sigma, x_{\mathcal{K}^*}]$ where σ denote an edge of $\mathcal{K}$ that admits $x_{\mathcal{K}^*}$ as vertex. The point x_σ denotes the center of σ. This construction is usually called the* barycentric dual mesh. *We do not choose such an approach here since the introduction of the m-DDFV method in this framework is a little bit more intricate. Nevertheless, in some particular geometric situations, we need to consider the* barycentric dual mesh *(see for instance Remark 2.4).*

For all neighbor control volumes $\mathcal{K}$ and $\mathcal{L}$, we assume that $\partial\mathcal{K} \cap \partial\mathcal{L}$ is an edge of the primal mesh denoted by $\sigma = \mathcal{K}|\mathcal{L}$. We note by $\mathcal{E}$ the set of such edges. We also note $\sigma^* = \mathcal{K}^*|\mathcal{L}^*$ and $\mathcal{E}^*$ for the corresponding dual definitions.

Given the primal and dual control volumes, we define the diamond cells $\mathcal{D}_{\sigma,\sigma^*}$ being the quadrangles whose diagonals are a primal edge $\sigma = \mathcal{K}|\mathcal{L} = (x_{\mathcal{K}^*}, x_{\mathcal{L}^*})$ and a corresponding dual edge $\sigma^* = \mathcal{K}^*|\mathcal{L}^* = (x_{\mathcal{K}}, x_{\mathcal{L}})$, (see Fig. 2.2). Note that the diamond cells are not necessarily convex. If $\sigma \in \mathcal{E} \cap \partial\overline{\Omega}$, the quadrangle $\mathcal{D}_{\sigma,\sigma^*}$ degenerate into a triangle. The set of the diamond cells is denoted by $\mathfrak{D}$ and we have $\overline{\Omega} = \bigcup_{\mathcal{D} \in \mathfrak{D}} \overline{\mathcal{D}}$.

Notations:
For any primal control volume $\mathcal{K} \in \mathfrak{M} \cap \partial\mathfrak{M}$, we note

- $m_{\mathcal{K}}$ its Lebesgue measure,
- $\mathcal{E}_{\mathcal{K}}$ the set of its edges (if $\mathcal{K} \in \mathfrak{M}$), or the one-element set $\{\mathcal{K}\}$ if $\mathcal{K} \in \partial\mathfrak{M}$.
- $\mathfrak{D}_{\mathcal{K}} = \{\mathcal{D}_{\sigma,\sigma^*} \in \mathfrak{D},\ \sigma \in \mathcal{E}_{\mathcal{K}}\}$,

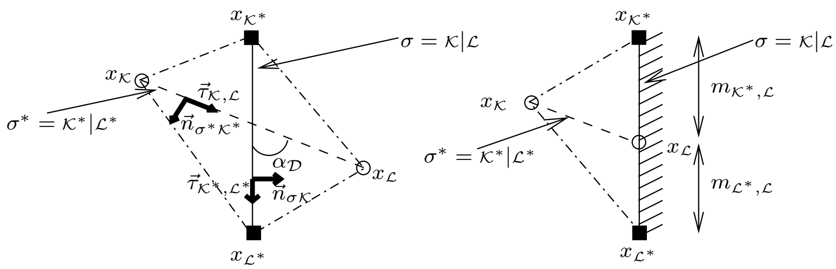

FIG. 2.2. Notations in the diamond cells. (Left) Interior cell. (Right) Boundary cell.

- $\vec{n}_{\mathcal{K}}$ the outward unit normal vector to $\mathcal{K}$.

We will also use corresponding dual notations: $m_{\mathcal{K}^*}$, $\mathcal{E}_{\mathcal{K}^*}$, $\mathfrak{D}_{\mathcal{K}^*}$ and $\vec{n}_{\mathcal{K}^*}$.
For a diamond cell $\mathcal{D} = \mathcal{D}_{\sigma,\sigma^*}$ whose vertices are $(x_{\mathcal{K}}, x_{\mathcal{K}^*}, x_{\mathcal{L}}, x_{\mathcal{L}^*})$, we note

- $x_{\mathcal{D}}$ the center of the diamond cell $\mathcal{D}$, that is the intersection of the primal edge σ and the dual edge σ^*,
- $m_{\mathcal{D}}$ its measure,
- m_σ the length of the primal edge σ,
- m_{σ^*} the length of the dual edge σ^*,
- $\vec{n}_{\sigma\mathcal{K}}$ the unit vector normal to σ oriented from $x_{\mathcal{K}}$ to $x_{\mathcal{L}}$,
- $\vec{n}_{\sigma^*\mathcal{K}^*}$ the unit vector normal to σ^* oriented from $x_{\mathcal{K}^*}$ to $x_{\mathcal{L}^*}$,
- $\vec{\tau}_{\mathcal{K},\mathcal{L}}$ the unit vector parallel to σ^* (oriented from $x_{\mathcal{K}}$ to $x_{\mathcal{L}}$),
- $\vec{\tau}_{\mathcal{K}^*,\mathcal{L}^*}$ the unit vector parallel to σ (oriented from $x_{\mathcal{K}^*}$ to $x_{\mathcal{L}^*}$),
- $\alpha_{\mathcal{D}}$ the angle between $\vec{\tau}_{\mathcal{K},\mathcal{L}}$ and $\vec{\tau}_{\mathcal{K}^*,\mathcal{L}^*}$, and $m_{\mathcal{K}^*,\mathcal{L}}$ (respectively $m_{\mathcal{L}^*,\mathcal{L}}$) the length between $x_{\mathcal{K}^*}$ (respectively $x_{\mathcal{L}^*}$) and $x_{\mathcal{L}}$ for any boundary degenerate diamond cell.
- $m_{\sigma\mathcal{K}}$ (respectively $m_{\sigma\mathcal{L}}$) the length between $x_{\mathcal{K}}$ (respectively $x_{\mathcal{L}}$) and $x_{\mathcal{D}}$,
- $m_{\sigma_{\mathcal{K}^*}}$ (respectively $m_{\sigma_{\mathcal{L}^*}}$) the length between $x_{\mathcal{K}^*}$ (respectively $x_{\mathcal{L}^*}$) and $x_{\mathcal{D}}$,
- $\mathcal{D}_{\mathcal{K}} = \mathcal{D} \cap \mathcal{K}$ the intersection of the diamond $\mathcal{D}$ and the primal control volume $\mathcal{K}$.

The boundary unit normal vectors are denoted by $\vec{n}^{\mathfrak{D}} \in (\mathbb{R}^2)^{\mathfrak{D}}$ such that $\vec{n}^{\mathcal{D}} = \vec{n}_{\sigma\mathcal{K}}$. We have to differentiate the interior diamond cells to the different boundary diamond cells by introducing the sets

- $\mathfrak{D}_{ext} = \{\mathcal{D} \in \mathfrak{D},\ \mathcal{D} \cap \partial\Omega \neq \emptyset\}$,
- $\mathfrak{D}_{int} = \mathfrak{D} \backslash \mathfrak{D}_{ext}$,
- $\mathfrak{D}_{\Gamma} = \{\mathcal{D} \in \mathfrak{D},\ \mathcal{D} \cap \Gamma \neq \emptyset\}$.

REMARK 2.2 *For all* $\mathcal{D} \in \mathfrak{D}_{ext}$*, we have* $m_{\sigma_{\mathcal{K}^*}} = m_{\mathcal{K}^*,\mathcal{L}}$ *and* $m_{\sigma_{\mathcal{L}^*}} = m_{\mathcal{L}^*,\mathcal{L}}$.

Finally we denote by $f_{\mathcal{K}}$ (resp. $f_{\mathcal{K}^*}$) the mean-value of the source term f on $\mathcal{K} \in \mathfrak{M}$ (resp. on $\mathcal{K}^* \in \mathfrak{M}^* \cup \partial\mathfrak{M}^*$). The family $((h_{\mathcal{K}})_{\mathcal{K}\in\partial\mathfrak{M}}, (h_{\mathcal{K}^*})_{\mathcal{K}^*\in\partial\mathfrak{M}^*})$ is also defined by:

$$h_{\mathcal{K}} = \frac{1}{m_{B_{\mathcal{K}}}} \int_{B_{\mathcal{K}}} h(s)\mathrm{d}s,\ \forall \mathcal{K} \in \partial\mathfrak{M}, \quad \text{and} \quad h_{\mathcal{K}^*} = \frac{1}{m_{B_{\mathcal{K}^*}}} \int_{B_{\mathcal{K}^*}} h(s)\mathrm{d}s,\ \forall \mathcal{K}^* \in \partial\mathfrak{M}^*.$$

Here $B_{\mathcal{K}} = B(x_{\mathcal{K}}, \rho_{\mathcal{K}}) \cap \partial\Omega$ and $B_{\mathcal{K}^*} = B(x_{\mathcal{K}^*}, \rho_{\mathcal{K}^*}) \cap \partial\Omega$ and $\rho_{\mathcal{K}}$ and $\rho_{\mathcal{K}^*}$ are positive numbers associated to the mesh $\mathcal{T}$ and such that $B_{\mathcal{K}} \subset \overline{\mathcal{K}}$ and $B_{\mathcal{K}^*} \subset \partial\mathcal{K}^*$.

REMARK 2.3 *In practice, during implementation, we do not construct explicitly the dual mesh. We only construct a diamond cell structure, which contains the information of vertices and centers that define a diamond cell. This structure also contains the measures of $\mathcal{D} \cap \mathcal{K}$, $\mathcal{D} \cap \mathcal{K}^*$ and the normal vectors $m_\sigma \vec{n}_{\sigma\mathcal{K}}$, $m_{\sigma^*}\vec{n}_{\sigma^*\mathcal{K}^*}$. If one uses the* barycentric dual mesh *instead of the above definition of the dual mesh (see Remark 2.1), then the natural choice for the center $x_{\mathcal{D}}$ of the diamond cell $\mathcal{D}$ is not the diagonal intersection but the middle x_σ of the edge σ. In that case, the above definitions have to be modified accordingly.*

The matrix of the discrete problem can then be completely assembled by using only this data structure.

From now on, for simplicity reasons, we will make the following assumption.

HYPOTHESIS 2.1 *We assume that diamond cells $\mathcal{D}$ are convex.*

This hypothesis implies that the center $x_{\mathcal{D}}$ of the diamond cell $\mathcal{D}$ (resp. the node $x_{\mathcal{K}^*}$ of the dual cell $\mathcal{K}^*$) lies inside $\mathcal{D}$ (resp. $\mathcal{K}^*$). We also have for all $\mathcal{D} \in \mathfrak{D}_{ext}$ that $m_{\sigma_{\mathcal{K}^*}} \geqslant 0$ and $m_{\sigma_{\mathcal{L}^*}} \geqslant 0$, and for all $(\mathcal{K}^*, \mathcal{L}^*) \in \mathfrak{M}^* \cup \partial\mathfrak{M}^*$ such that $\mathcal{K}^* \neq \mathcal{L}^*$, we have $\overset{\circ}{\widehat{\mathcal{K}^*}} \cap \overset{\circ}{\widehat{\mathcal{L}^*}} = \emptyset$.

REMARK 2.4 *If the hypothesis 2.1 is not satisfied, for instance as in Figure 2.3, it is needed, at least for those of the diamonds that are not convex, to take the* barycentric dual mesh *(see Remark 2.1) and then to define the center $x_{\mathcal{D}}$ of this diamond cell $\mathcal{D}_{\sigma,\sigma^*}$ as the middle of the edge σ. Remarks 3.1 and 4.2 specify how to adapt the Schwarz algorithm in this case.*

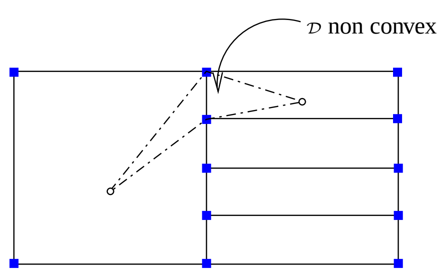

FIG. 2.3. An example where the diamond cells $\mathcal{D}$ could be non convex.

The unknowns: the m-DDFV method associates to all primal control volumes $\mathcal{K} \in \mathfrak{M} \cup \partial\mathfrak{M}$ an unknown value $u_{\mathcal{K}}$ and to all dual control volumes $\mathcal{K}^* \in \mathfrak{M}^* \cup \partial\mathfrak{M}^*$ an unknown value $u_{\mathcal{K}^*}$. We denote the approximate solution on the mesh $\mathcal{T}$ by $u^{\mathcal{T}} \in \mathbb{R}^{\mathcal{T}}$ where

$$u^{\mathcal{T}} = \Big((u_{\mathcal{K}})_{\mathcal{K}\in(\mathfrak{M}\cup\partial\mathfrak{M})}, (u_{\mathcal{K}^*})_{\mathcal{K}^*\in(\mathfrak{M}^*\cup\partial\mathfrak{M}^*)} \Big).$$

Inner products: we define the two following inner products

$$[\![v^{\mathcal{T}}, u^{\mathcal{T}}]\!]_{\mathcal{T}} = \frac{1}{2}\left(\sum_{\mathcal{K}\in\mathfrak{M}} m_{\mathcal{K}} u_{\mathcal{K}} v_{\mathcal{K}} + \sum_{\mathcal{K}^*\in(\mathfrak{M}^*\cup\partial\mathfrak{M}^*)} m_{\mathcal{K}^*} u_{\mathcal{K}^*} v_{\mathcal{K}^*}\right), \quad \forall u^{\mathcal{T}}, v^{\mathcal{T}} \in \mathbb{R}^{\mathcal{T}}, \tag{2.1}$$

$$(\xi^{\mathfrak{D}}, \eta^{\mathfrak{D}})_{\mathfrak{D}} = \sum_{\mathcal{D}\in\mathfrak{D}} m_{\mathcal{D}} \xi^{\mathcal{D}} \cdot \eta^{\mathcal{D}}, \quad \forall \xi^{\mathfrak{D}}, \eta^{\mathfrak{D}} \in (\mathbb{R}^2)^{\mathfrak{D}},$$

and the corresponding norm

$$||\xi^{\mathfrak{D}}||_{\mathfrak{D}}^2 = (\xi^{\mathfrak{D}}, \xi^{\mathfrak{D}})_{\mathfrak{D}}, \quad \forall \xi^{\mathfrak{D}} \in (\mathbb{R}^2)^{\mathfrak{D}}.$$

Boundary inner products: we define the following L^2 inner product on the boundary of Ω

$$(u^{\mathfrak{D}}, v^{\mathfrak{D}})_{\partial\Omega} = \sum_{\mathcal{D}_{\sigma,\sigma^*}\in\mathfrak{D}_{ext}} m_\sigma u^{\mathcal{D}} \cdot v^{\mathcal{D}}, \quad \forall u^{\mathfrak{D}}, v^{\mathfrak{D}} \in \mathbb{R}^{\mathfrak{D}}.$$

Trace operators: we will need the following definition of a trace operator in the DDFV framework

$$\gamma^{\mathcal{T}}(u^{\mathcal{T}}) = \left(\gamma^{\mathcal{D}}(u^{\mathcal{T}})\right)_{\mathcal{D}\in\mathfrak{D}}, \quad \forall u^{\mathcal{T}} \in \mathbb{R}^{\mathcal{T}},$$

where

$$\gamma^{\mathcal{D}}(u^{\mathcal{T}}) = \frac{m_{\mathcal{K}^*,\mathcal{L}}}{m_\sigma}\gamma_{\mathcal{K}^*,\mathcal{L}}(u^{\mathcal{T}}) + \frac{m_{\mathcal{L}^*,\mathcal{L}}}{m_\sigma}\gamma_{\mathcal{L}^*,\mathcal{L}}(u^{\mathcal{T}}) \qquad \text{and} \qquad \gamma_{\mathcal{K}^*,\mathcal{L}}(u^{\mathcal{T}}) = \frac{u_{\mathcal{K}^*} + u_{\mathcal{L}}}{2} \tag{2.2}$$

Discrete gradient: we define (like in [6, 12]) a consistent approximation of the gradient operator denoted by $\nabla^{\mathfrak{D}} : u^{\mathcal{T}} \in \mathbb{R}^{\mathcal{T}} \mapsto (\nabla^{\mathcal{D}} u^{\mathcal{T}})_{\mathcal{D}\in\mathfrak{D}} \in (\mathbb{R}^2)^{\mathfrak{D}}$, as follows:

$$\nabla^{\mathcal{D}} u^{\mathcal{T}} = \frac{1}{2m_{\mathcal{D}}}\left[(u_{\mathcal{L}} - u_{\mathcal{K}}) m_\sigma \vec{n}_{\sigma\mathcal{K}} + (u_{\mathcal{L}^*} - u_{\mathcal{K}^*}) m_{\sigma^*} \vec{n}_{\sigma^*\mathcal{K}^*}\right], \quad \forall \mathcal{D} \in \mathfrak{D}. \tag{2.3}$$

Discrete divergence: we define a consistent approximation of the divergence operator denoted by $\mathrm{div}^{\mathcal{T}} : \xi = (\xi^{\mathcal{D}})_{\mathcal{D}\in\mathfrak{D}} \mapsto \mathrm{div}^{\mathcal{T}}\xi \in \mathbb{R}^{\mathcal{T}}$, as follows:

$$\mathrm{div}^{\mathcal{K}}\xi = \frac{1}{m_{\mathcal{K}}} \sum_{\mathcal{D}\in\mathfrak{D}_{\mathcal{K}}} m_\sigma(\xi^{\mathcal{D}}, \vec{n}_{\sigma\mathcal{K}}), \ \forall \mathcal{K} \in \mathfrak{M}, \ \text{ and } \ \mathrm{div}^{\mathcal{K}}\xi = 0, \ \forall \mathcal{K} \in \partial\mathfrak{M}, \tag{2.4a}$$

$$\mathrm{div}^{\mathcal{K}^*}\xi = \frac{1}{m_{\mathcal{K}^*}} \sum_{\mathcal{D}\in\mathfrak{D}_{\mathcal{K}^*}} m_{\sigma^*}(\xi^{\mathcal{D}}, \vec{n}_{\sigma^*\mathcal{K}^*}), \ \forall \mathcal{K}^* \in \mathfrak{M}^*, \tag{2.4b}$$

$$\mathrm{div}^{\mathcal{K}^*}\xi = \frac{1}{m_{\mathcal{K}^*}}\left(\sum_{\mathcal{D}\in\mathfrak{D}_{\mathcal{K}^*}} m_{\sigma^*}(\xi^{\mathcal{D}}, \vec{n}_{\sigma^*\mathcal{K}^*}) + \sum_{\substack{\mathcal{D}\in\mathfrak{D}_{\mathcal{K}^*} \\ \mathcal{D}\cap\partial\Omega\neq\emptyset}} m_{\mathcal{K}^*,\mathcal{L}}(\xi^{\mathcal{D}}, \vec{n}_{\sigma\mathcal{K}})\right), \quad \forall \mathcal{K}^* \in \partial\mathfrak{M}^*. \tag{2.4c}$$

These two operators are in *discrete duality* (giving its name to the scheme) since it is possible to prove a discrete Stokes formula using these two operators (see for instance [2, 5, 6]).

THEOREM 2.1 (STOKES FORMULA) *For any $\xi^{\mathfrak{D}} \in (\mathbb{R}^2)^{\mathfrak{D}}$, $u^{\mathcal{T}} \in \mathbb{R}^{\mathcal{T}}$, we have*

$$[\![\mathrm{div}^{\mathcal{T}}(\xi^{\mathfrak{D}}), u^{\mathcal{T}}]\!]_{\mathcal{T}} = -(\xi^{\mathfrak{D}}, \nabla^{\mathfrak{D}} u^{\mathcal{T}})_{\mathfrak{D}} + (\xi^{\mathfrak{D}} \cdot \vec{n}^{\mathfrak{D}}, \gamma^{\mathcal{T}}(u^{\mathcal{T}}))_{\partial\Omega}. \tag{2.5}$$

3. The m-DDFV scheme with mixed Dirichlet/Fourier boundary conditions

We consider problem (1.1) and we assume that the primal mesh is chosen in such a (natural) way that $\partial\Gamma \subset X^*$. We note : $\partial\mathfrak{M}_D = \{\kappa \in \partial\mathfrak{M}, x_\kappa \notin \Gamma\}$, $\partial\mathfrak{M}_\Gamma = \{\kappa \in \partial\mathfrak{M}, x_\kappa \in \Gamma\}$, $\partial\mathfrak{A}_\Gamma = \{$The half-edges belonging to Γ, $[x_{\kappa^*}x_{\mathcal{L}}] \subset \mathcal{L} \in \partial\mathfrak{M}_\Gamma\}$, $\partial\mathfrak{M}^*_D = \{\kappa^* \in \partial\mathfrak{M}^*, x_{\kappa^*} \in \partial\Omega\backslash\Gamma\} \cup \{\kappa^* \in \partial\mathfrak{M}^*, x_{\kappa^*} \in \partial\Gamma\}$, $\partial\mathfrak{M}^*_\Gamma = \{\kappa^* \in \partial\mathfrak{M}^*, x_{\kappa^*} \in \Gamma$ and $x_{\kappa^*} \notin \partial\Gamma\}$. We now introduce two new flux unknowns $\varphi_{\kappa^*,\mathcal{L}}$ and $\varphi_{\mathcal{L}^*,\mathcal{L}}$ for each degenerate boundary control volume $\mathcal{L} = [x_{\kappa^*}x_{\mathcal{L}^*}]$ belonging to $\partial\mathfrak{M}_\Gamma$. These two unknowns are meant to approximate $(A\nabla u, \vec{n}_{\sigma\mathcal{L}})$ along respectively $[x_{\kappa^*}, x_{\mathcal{L}}]$ and $[x_{\mathcal{L}}, x_{\mathcal{L}^*}]$. Notice that there are other, somewhat more simple, ways to deal with Fourier boundary conditions in the m-DDFV framework but the introduction of these additional unknowns is needed to be able to build a convergent non-overlapping Schwarz iterative method, which is our main objective in this paper (see Section 4).

Let us denote by $\Phi^{\mathcal{T}}_\Gamma$ the set of these new unknowns

$$\Phi^{\mathcal{T}}_\Gamma = \left\{\phi^{\mathcal{T}} = (\varphi_{\kappa^*,\mathcal{L}}, \varphi_{\mathcal{L}^*,\mathcal{L}})_{\mathcal{L}=[x_{\kappa^*}x_{\mathcal{L}^*}]\in\partial\mathfrak{M}_\Gamma}\right\}.$$

The new approximate m-DDFV solution is now a couple $U^{\mathcal{T}} = (u^{\mathcal{T}}, \phi^{\mathcal{T}}) \in \mathbb{R}^{\mathcal{T}} \times \Phi^{\mathcal{T}}_\Gamma$ solving the following set of linear equations:

$$-\text{div}^{\kappa}\left(A^{\mathfrak{D}}\nabla^{\mathfrak{D}}u^{\mathcal{T}}\right) = f_\kappa,\ \ \forall\, \kappa \in \mathfrak{M}, \tag{3.1a}$$

$$-\text{div}^{\kappa^*}\left(A^{\mathfrak{D}}\nabla^{\mathfrak{D}}u^{\mathcal{T}}\right) = f_{\kappa^*},\ \ \forall\, \kappa^* \in \mathfrak{M}^*, \tag{3.1b}$$

$$-\sum_{\mathcal{D}\in\mathfrak{D}_{\kappa^*}}\frac{m_{\sigma^*}}{m_{\kappa^*}}\left(A_{\mathcal{D}}\nabla^{\mathcal{D}}u^{\mathcal{T}}, \vec{n}_{\sigma^*\kappa^*}\right) - \sum_{\substack{\mathcal{D}\in\mathfrak{D}_{\kappa^*}\\ \mathcal{D}\cap\Gamma\neq\emptyset}}\frac{m_{\kappa^*,\mathcal{L}}}{m_{\kappa^*}}\varphi_{\kappa^*,\mathcal{L}} = f_{\kappa^*},\quad \forall\ \kappa^* \in \partial\mathfrak{M}^*_\Gamma, \tag{3.1c}$$

$$\frac{m_{\kappa^*,\mathcal{L}}}{m_\sigma}\varphi_{\kappa^*,\mathcal{L}} + \frac{m_{\mathcal{L}^*,\mathcal{L}}}{m_\sigma}\varphi_{\mathcal{L}^*,\mathcal{L}} = \left(A_{\mathcal{D}}\nabla^{\mathcal{D}}u^{\mathcal{T}}, \vec{n}_{\sigma\mathcal{L}}\right),\ \ \forall\, \mathcal{L} = [x_{\kappa^*}x_{\mathcal{L}^*}] \in \partial\mathfrak{M}_\Gamma, \tag{3.1d}$$

$$u_\kappa = h_\kappa,\ \ \forall\, \kappa \in \partial\mathfrak{M}_D, \qquad u_{\kappa^*} = h_{\kappa^*},\ \ \forall\, \kappa^* \in \partial\mathfrak{M}^*_D, \tag{3.1e}$$

$$\varphi_{\kappa^*,\mathcal{L}} + \lambda\frac{u_{\kappa^*} + u_{\mathcal{L}}}{2} = g_{\kappa^*,\mathcal{L}},\ \ \forall\, [x_{\kappa^*}x_{\mathcal{L}}] \in \partial\mathfrak{A}_\Gamma, \tag{3.1f}$$

where $A^{\mathfrak{D}} = (A_{\mathcal{D}})_{\mathcal{D}\in\mathfrak{D}}$, $A_{\mathcal{D}}$ is a definite positive matrix which approximates A on the diamond $\mathcal{D}$.

In order to simplify the notations a little, we will now denote the fact that $U^{\mathcal{T}}{=}(u^{\mathcal{T}}, \phi^{\mathcal{T}}) \in \mathbb{R}^{\mathcal{T}} \times \Phi^{\mathcal{T}}_\Gamma$ solves (3.1), for some data $(f^{\mathcal{T}}, h^{\mathcal{T}}, g^{\mathcal{T}})$, in the following compact way

$$\mathcal{L}^{\mathcal{T}}_{\Omega,\Gamma}(u^{\mathcal{T}}, \phi^{\mathcal{T}}, f^{\mathcal{T}}, h^{\mathcal{T}}, g^{\mathcal{T}}) = 0.$$

The above m-DDFV finite volume scheme is obtained by formally integrating the equation (1.1) on each interior primal control volumes (3.1a), on interior dual control volumes (3.1b) and also on boundary dual control volumes belonging to $\partial\mathfrak{M}^*_\Gamma$ (3.1c). The numerical fluxes are approximated by using the discrete gradient operator $\nabla^{\mathcal{D}}$ for edges lying inside the domain or on $\partial\Omega \setminus \Gamma$, and by using the flux unknowns $\phi^{\mathcal{T}}$ on Γ.

We link up these unknowns $\phi^{\mathcal{T}}$ to the discrete m-DDFV gradient on each Fourier boundary control volumes by equation (3.1d). Finally, we impose the Dirichlet boundary condition on the boundary primal control volumes belonging to $\partial\mathfrak{M}_D$ and on boundary dual control volumes belonging to $\partial\mathfrak{M}^*_D$ (3.1e) and we impose the Fourier boundary condition using the flux unknowns $\phi^{\mathcal{T}}$ on each half-edge lying into Γ (3.1f), $g_{\kappa^*,\mathcal{L}}$ being a discrete boundary Fourier data which can be, for instance, the mean-value of a function g on $[x_{\kappa^*}x_{\mathcal{L}}]$.

There exist many possibilities to define the matrix $A_{\mathcal{D}}$. We mainly consider the two following cases.

- If A is smooth with respect to the space variable x, *i.e.* there exists $C_A > 0$ such that:

$$\|A(x) - A(x')\| \leqslant C_A|x - x'|, \quad \forall x, x' \in \Omega,$$

  we choose, for example, to take $A_{\mathcal{D}} = A(x_{\mathcal{D}})$, for any $\mathcal{D} \in \mathfrak{D}$.

- If A is possibly discontinuous across primal or dual edges in the mesh, then a good choice for $A^{\mathfrak{D}}$ is more intricate. We recall here the main lines of the so-called m-DDFV scheme (see [12, 3]). In the case where $A(x)$ is constant on each primal control volume, we denote by $A_{\mathcal{K}}$ the value $A(x)$ on the control volume $\mathcal{K}$. For all $\mathcal{D} \in \mathfrak{D}_{ext}$, we choose $A_{\mathcal{D}}$ to be equal to $A_{\mathcal{K}}$ where $\mathcal{K}$ is the unique primal control volume such that $\mathcal{D} \subset \mathcal{K}$, and for all $\mathcal{D} \in \mathfrak{D}_{int}$, we define $A_{\mathcal{D}}$ by the following formulas

$$(A_{\mathcal{D}}\vec{n}_{\mathcal{K}}, \vec{n}_{\mathcal{K}}) = \frac{m_{\sigma^*}(A_{\mathcal{K}}\vec{n}_{\mathcal{K}}, \vec{n}_{\mathcal{K}})(A_{\mathcal{L}}\vec{n}_{\mathcal{K}}, \vec{n}_{\mathcal{K}})}{m_{\sigma_{\mathcal{L}}}(A_{\mathcal{K}}\vec{n}_{\mathcal{K}}, \vec{n}_{\mathcal{K}}) + m_{\sigma_{\mathcal{K}}}(A_{\mathcal{L}}\vec{n}_{\mathcal{K}}, \vec{n}_{\mathcal{K}})}, \tag{3.2a}$$

$$\begin{aligned}(A_{\mathcal{D}}\vec{n}_{\mathcal{K}^*}, \vec{n}_{\mathcal{K}^*}) =& \frac{m_{\sigma_{\mathcal{L}}}(A_{\mathcal{L}}\vec{n}_{\mathcal{K}^*}, \vec{n}_{\mathcal{K}^*}) + m_{\sigma_{\mathcal{K}}}(A_{\mathcal{K}}\vec{n}_{\mathcal{K}^*}, \vec{n}_{\mathcal{K}^*})}{m_{\sigma^*}} \\ &- \frac{m_{\sigma_{\mathcal{K}}}m_{\sigma_{\mathcal{L}}}}{m_{\sigma^*}} \frac{((A_{\mathcal{K}}\vec{n}_{\mathcal{K}}, \vec{n}_{\mathcal{K}^*}) - (A_{\mathcal{L}}\vec{n}_{\mathcal{K}}, \vec{n}_{\mathcal{K}^*}))^2}{m_{\sigma_{\mathcal{L}}}(A_{\mathcal{K}}\vec{n}_{\mathcal{K}}, \vec{n}_{\mathcal{K}}) + m_{\sigma_{\mathcal{K}}}(A_{\mathcal{L}}\vec{n}_{\mathcal{K}}, \vec{n}_{\mathcal{K}})},\end{aligned} \tag{3.2b}$$

$$(A_{\mathcal{D}}\vec{n}_{\mathcal{K}}, \vec{n}_{\mathcal{K}^*}) = \frac{m_{\sigma_{\mathcal{L}}}(A_{\mathcal{L}}\vec{n}_{\mathcal{K}}, \vec{n}_{\mathcal{K}^*})(A_{\mathcal{K}}\vec{n}_{\mathcal{K}}, \vec{n}_{\mathcal{K}}) + m_{\sigma_{\mathcal{K}}}(A_{\mathcal{K}}\vec{n}_{\mathcal{K}}, \vec{n}_{\mathcal{K}^*})(A_{\mathcal{L}}\vec{n}_{\mathcal{K}}, \vec{n}_{\mathcal{K}})}{m_{\sigma_{\mathcal{L}}}(A_{\mathcal{K}}\vec{n}_{\mathcal{K}}, \vec{n}_{\mathcal{K}}) + m_{\sigma_{\mathcal{K}}}(A_{\mathcal{L}}\vec{n}_{\mathcal{K}}, \vec{n}_{\mathcal{K}})}. \tag{3.2c}$$

  We recognize in (3.2a) the weighted harmonic mean-value of $(A_{\mathcal{K}}\vec{n}_{\mathcal{K}}, \vec{n}_{\mathcal{K}})$ and $(A_{\mathcal{L}}\vec{n}_{\mathcal{K}}, \vec{n}_{\mathcal{K}})$ and in the first term of (3.2b) the weighted arithmetic mean-value of $(A_{\mathcal{K}}\vec{n}_{\mathcal{K}^*}, \vec{n}_{\mathcal{K}^*})$ and $(A_{\mathcal{L}}\vec{n}_{\mathcal{K}^*}, \vec{n}_{\mathcal{K}^*})$. This particular choice of $A^{\mathfrak{D}}$ ensures the consistency of the discrete normal flux on each edges of primal and dual meshes.

REMARK 3.1 (BARYCENTRIC DUAL MESH) *In the case we use the* barycentric dual mesh, *the computations leading to those formulas can be obviously adapted (see [12]). We find that formula* (3.2a) *is unchanged and that formulas* (3.2b) *and* (3.2c) *change as follows (using notations of Figure 3.1):*

$$\begin{aligned}(A_{\mathcal{D}}\vec{n}_{\sigma^*\mathcal{K}^*}, \vec{n}_{\sigma^*\mathcal{K}^*}) =& \frac{m_{\sigma_2^*}(A_{\mathcal{L}}\vec{n}_{\sigma_2^*\mathcal{K}^*}, \vec{n}_{\sigma_2^*\mathcal{K}^*})\frac{m_{\sigma_2^*}}{m_{\sigma_{\mathcal{L}}}} + m_{\sigma_1^*}(A_{\mathcal{K}}\vec{n}_{\sigma_1^*\mathcal{K}^*}, \vec{n}_{\sigma_1^*\mathcal{K}^*})\frac{m_{\sigma_1^*}}{m_{\sigma_{\mathcal{K}}}}}{m_{\sigma^*}} \\ &- \frac{m_{\sigma_{\mathcal{K}}}m_{\sigma_{\mathcal{L}}}\left(A_{\mathcal{L}}\frac{m_{\sigma_2^*}}{m_{\sigma_{\mathcal{L}}}}\vec{n}_{\sigma_2^*\mathcal{K}^*} - A_{\mathcal{K}}\frac{m_{\sigma_1^*}}{m_{\sigma_{\mathcal{K}}}}\vec{n}_{\sigma_1^*\mathcal{K}^*}, \vec{n}_{\sigma\mathcal{K}}\right)^2}{m_{\sigma^*}\left((A_{\mathcal{K}}m_{\sigma_{\mathcal{L}}} + A_{\mathcal{L}}m_{\sigma_{\mathcal{K}}})\vec{n}_{\sigma\mathcal{K}}, \vec{n}_{\sigma\mathcal{K}}\right)},\end{aligned} \tag{3.2b-bis}$$

$$(A_{\mathcal{D}}\vec{n}_{\sigma\mathcal{K}}, \vec{n}_{\sigma^*\mathcal{K}^*}) = \frac{m_{\sigma_2^*}(A_{\mathcal{K}}\vec{n}_{\sigma\mathcal{K}}, \vec{n}_{\sigma\mathcal{K}})\left(A_{\mathcal{L}}\vec{n}_{\sigma_2^*\mathcal{K}^*}, \vec{n}_{\sigma\mathcal{K}}\right) + m_{\sigma_1^*}(A_{\mathcal{L}}\vec{n}_{\sigma\mathcal{K}}, \vec{n}_{\sigma\mathcal{K}})\left(A_{\mathcal{K}}\vec{n}_{\sigma_1^*\mathcal{K}^*}, \vec{n}_{\sigma\mathcal{K}}\right)}{m_{\sigma_{\mathcal{L}}}(A_{\mathcal{K}}\vec{n}_{\sigma\mathcal{K}}, \vec{n}_{\sigma\mathcal{K}}) + m_{\sigma_{\mathcal{K}}}(A_{\mathcal{L}}\vec{n}_{\sigma\mathcal{K}}, \vec{n}_{\sigma\mathcal{K}})}, \tag{3.2c-bis}$$

with $\vec{n}_{\sigma^*\mathcal{K}^*} = \vec{n}_{\mathcal{K}^*}$ *and* $\vec{n}_{\sigma\mathcal{K}} = \vec{n}_{\mathcal{K}}$.

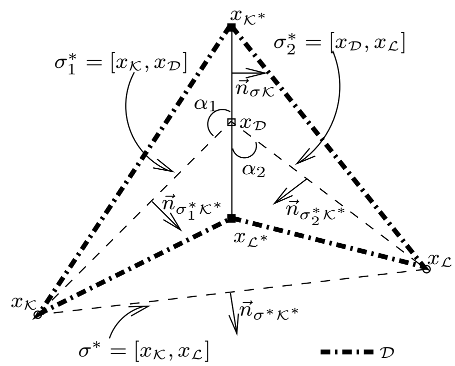

FIG. 3.1. Notation for a diamond cell whose center $x_{\mathcal{D}}$ is the middle of $\sigma = [x_{\mathcal{K}^*}, x_{\mathcal{L}^*}]$.

As shown in [3], this particular choice for $A^{\mathfrak{D}}$ imply a first order convergence of the scheme in the case of Dirichlet boundary conditions. More precisely, if we introduce the space $H^2(\mathfrak{M}) = \{u \in H_0^1(\Omega), u_{|\mathcal{K}} \in H^2(\kappa),\ \forall \kappa \in \mathfrak{M}\}$, the following theorem is proved in [3]:

THEOREM 3.1 (ERROR ESTIMATE FOR M-DDFV, DIRICHLET BOUNDARY CONDITIONS) *Assume that the exact solution u, to the problem* (1.1) *with $\Gamma = \emptyset$, lies in $H^2(\mathfrak{M})$. Under suitable regularity assumptions on the meshes, $u^{\mathcal{T}}$ and $\nabla^{\mathfrak{D}} u^{\mathcal{T}}$ are first order approximations of u and ∇u, respectively, in the L^2 norm.*

In the case of Dirichlet/Fourier boundary conditions under study in this section, the error estimate of Theorem 3.1 can also be proved but we will not give the proof.

The main result of this section is the following existence and uniqueness theorem.

THEOREM 3.2 *The finite volume scheme* (3.1) *which approximates Problem* (1.1) *on a DDFV mesh $\mathcal{T}$ possesses a unique solution $U^{\mathcal{T}} = (u^{\mathcal{T}}, \phi^{\mathcal{T}}) \in \mathbb{R}^{\mathcal{T}} \times \Phi_\Gamma^{\mathcal{T}}$.*

We first give a technical Lemma which is useful in the proof of Theorem 3.2 and 4.2.

LEMMA 3.1 *For all $g^{\mathcal{T}} \in \Phi_\Gamma^{\mathcal{T}}$, and $U^{\mathcal{T}}=(u^{\mathcal{T}}, \phi^{\mathcal{T}}) \in \mathbb{R}^{\mathcal{T}} \times \Phi_\Gamma^{\mathcal{T}}$ such that*

$$\mathcal{L}_{\Omega,\Gamma}^{\mathcal{T}}(u^{\mathcal{T}}, \phi^{\mathcal{T}}, 0, 0, g^{\mathcal{T}}) = 0,$$

we have

$$-[\![div^{\mathcal{T}}(A^{\mathfrak{D}}\nabla^{\mathfrak{D}}u^{\mathcal{T}}), u^{\mathcal{T}}]\!]_{\mathcal{T}} = -\frac{\lambda}{4}\sum_{\mathcal{D}\in\mathfrak{D}_\Gamma} M_\sigma(u_{\mathcal{K}^*} - u_{\mathcal{L}^*})^2 - \frac{1}{2}\sum_{\mathcal{K}^*\in\partial\mathfrak{M}_\Gamma^*} u_{\mathcal{K}^*} \sum_{\substack{\mathcal{D}\in\mathfrak{D}_{\mathcal{K}^*}\\ \mathcal{D}\cap\Gamma\neq\emptyset}} M_\sigma(g_{\mathcal{L}^*,\mathcal{L}} - g_{\mathcal{K}^*,\mathcal{L}}),$$

where $M_\sigma = \frac{m_{\mathcal{K}^*,\mathcal{L}}\ m_{\mathcal{L}^*,\mathcal{L}}}{m_\sigma}$.

Proof. The vector $U^{\mathcal{T}} = (u^{\mathcal{T}}, \phi^{\mathcal{T}}) \in \mathbb{R}^{\mathcal{T}} \times \Phi_\Gamma^{\mathcal{T}}$ solves :

$$-\mathrm{div}^{\mathcal{K}}\,(A^{\mathfrak{D}}\nabla^{\mathfrak{D}}u^{\mathcal{T}}) = 0,\ \ \forall\, \kappa \in \mathfrak{M}, \tag{3.4a}$$

$$-\mathrm{div}^{\mathcal{K}^*}\,(A^{\mathfrak{D}}\nabla^{\mathfrak{D}}u^{\mathcal{T}}) = 0,\ \ \forall\, \kappa^* \in \mathfrak{M}^*, \tag{3.4b}$$

$$- \sum_{\mathcal{D}\in\mathfrak{D}_{\mathcal{K}^*}} \frac{m_{\sigma^*}}{m_{\mathcal{K}^*}} (A_{\mathcal{D}}\nabla^{\mathcal{D}} u^{\mathcal{T}}, \vec{n}_{\sigma^*\mathcal{K}^*}) - \sum_{\substack{\mathcal{D}\in\mathfrak{D}_{\mathcal{K}^*}\\ \mathcal{D}\cap\Gamma\neq\emptyset}} \frac{m_{\mathcal{K}^*,\mathcal{L}}}{m_{\mathcal{K}^*}} \varphi_{\mathcal{K}^*,\mathcal{L}} = 0, \quad \forall\ \mathcal{K}^* \in \partial\mathfrak{M}^*_{\Gamma}, \tag{3.4c}$$

$$\frac{m_{\mathcal{K}^*,\mathcal{L}}}{m_\sigma}\varphi_{\mathcal{K}^*,\mathcal{L}} + \frac{m_{\mathcal{L}^*,\mathcal{L}}}{m_\sigma}\varphi_{\mathcal{L}^*,\mathcal{L}} = (A_{\mathcal{D}}\nabla^{\mathcal{D}} u^{\mathcal{T}}, \vec{n}_{\sigma\mathcal{L}}),\ \forall\, \mathcal{L} = [x_{\mathcal{K}^*} x_{\mathcal{L}^*}] \in \partial\mathfrak{M}_{\Gamma}, \tag{3.4d}$$

$$u_{\mathcal{K}} = 0,\ \forall\, \mathcal{K} \in \partial\mathfrak{M}_D, \qquad u_{\mathcal{K}^*} = 0,\ \forall\, \mathcal{K}^* \in \partial\mathfrak{M}^*_D, \tag{3.4e}$$

$$\varphi_{\mathcal{K}^*,\mathcal{L}} + \lambda \frac{u_{\mathcal{K}^*} + u_{\mathcal{L}}}{2} = g_{\mathcal{K}^*,\mathcal{L}},\ \forall\, [x_{\mathcal{K}^*} x_{\mathcal{L}}] \in \partial\mathfrak{A}_{\Gamma}. \tag{3.4f}$$

Using the definition (2.1) of $[\![\cdot,\cdot]\!]_{\mathcal{T}}$ on Ω and successively (3.4a)-(3.4c) and (3.4d), then (3.4e) and finally (3.4f) it follows:

$$\begin{aligned}
-[\![\mathrm{div}^{\mathcal{T}}(A^{\mathfrak{D}}\nabla^{\mathfrak{D}} u^{\mathcal{T}}), u^{\mathcal{T}}]\!]_{\mathcal{T}} &= -\frac{1}{2}\sum_{\mathcal{K}^*\in\partial\mathfrak{M}^*_{\Gamma}} u_{\mathcal{K}^*} \sum_{\substack{\mathcal{D}\in\mathfrak{D}_{\mathcal{K}^*}\\ \mathcal{D}\cap\Gamma\neq\emptyset}} m_{\mathcal{K}^*,\mathcal{L}} \left((A_{\mathcal{D}}\nabla^{\mathcal{D}} u^{\mathcal{T}}, \vec{n}_{\sigma\mathcal{L}}) - \varphi_{\mathcal{K}^*,\mathcal{L}}\right)\\
&= -\frac{1}{2}\sum_{\mathcal{K}^*\in\partial\mathfrak{M}^*_{\Gamma}} u_{\mathcal{K}^*} \sum_{\substack{\mathcal{D}\in\mathfrak{D}_{\mathcal{K}^*}\\ \mathcal{D}\cap\Gamma\neq\emptyset}} \frac{m_{\mathcal{K}^*,\mathcal{L}} m_{\mathcal{L}^*,\mathcal{L}}}{m_\sigma} \left(\varphi_{\mathcal{L}^*,\mathcal{L}} - \varphi_{\mathcal{K}^*,\mathcal{L}}\right)\\
&= -\frac{1}{2}\sum_{\mathcal{K}^*\in\partial\mathfrak{M}^*_{\Gamma}} u_{\mathcal{K}^*} \sum_{\substack{\mathcal{D}\in\mathfrak{D}_{\mathcal{K}^*}\\ \mathcal{D}\cap\Gamma\neq\emptyset}} M_\sigma \lambda \left(\gamma_{\mathcal{K}^*,\mathcal{L}}(u^{\mathcal{T}}) - \gamma_{\mathcal{L}^*,\mathcal{L}}(u^{\mathcal{T}})\right)\\
&\quad -\frac{1}{2}\sum_{\mathcal{K}^*\in\partial\mathfrak{M}^*_{\Gamma}} u_{\mathcal{K}^*} \sum_{\substack{\mathcal{D}\in\mathfrak{D}_{\mathcal{K}^*}\\ \mathcal{D}\cap\Gamma\neq\emptyset}} M_\sigma \left(g_{\mathcal{L}^*,\mathcal{L}} - g_{\mathcal{K}^*,\mathcal{L}}\right).
\end{aligned}$$

The claim follows by noting that, since $\partial\Gamma \subset X^*$, the first term in the right hand side above can be written

$$\frac{1}{2}\sum_{\mathcal{K}^*\in\partial\mathfrak{M}^*_{\Gamma}} u_{\mathcal{K}^*} \sum_{\substack{\mathcal{D}\in\mathfrak{D}_{\mathcal{K}^*}\\ \mathcal{D}\cap\Gamma\neq\emptyset}} M_\sigma \frac{\lambda}{2}\left(u_{\mathcal{K}^*} - u_{\mathcal{L}^*}\right) = \frac{1}{2}\sum_{\mathcal{D}\in\mathfrak{D}_{\Gamma}} M_\sigma \frac{\lambda}{2}\left(u_{\mathcal{K}^*} - u_{\mathcal{L}^*}\right)^2.$$

□

We can now proceed to the proof of the Theorem 3.2.

Proof of the Theorem 3.2. The wellposedness of this square linear system is equivalent to showing that it has a trivial kernel. Let $U^{\mathcal{T}} = (u^{\mathcal{T}}, \phi^{\mathcal{T}}) \in \mathbb{R}^{\mathcal{T}} \times \Phi^{\mathcal{T}}_{\Gamma}$ which solves

$$\mathcal{L}^{\mathcal{T}}_{\Omega,\Gamma}(u^{\mathcal{T}}, \phi^{\mathcal{T}}, 0, 0, 0) = 0. \tag{3.5}$$

Using Lemma 3.1, we have :

$$-[\![\mathrm{div}^{\mathcal{T}}(A^{\mathfrak{D}}\nabla^{\mathfrak{D}} u^{\mathcal{T}}), u^{\mathcal{T}}]\!]_{\mathcal{T}} = -\frac{\lambda}{4}\sum_{\mathcal{D}\in\mathfrak{D}_{\Gamma}} M_\sigma (u_{\mathcal{K}^*} - u_{\mathcal{L}^*})^2.$$

The discrete Stokes formula (2.5) gives:

$$\begin{aligned}
-[\![\mathrm{div}^{\mathcal{T}}(A^{\mathfrak{D}}\nabla^{\mathfrak{D}} u^{\mathcal{T}}), u^{\mathcal{T}}]\!]_{\mathcal{T}} &= (A^{\mathfrak{D}}\nabla^{\mathfrak{D}} u^{\mathcal{T}}, \nabla^{\mathfrak{D}} u^{\mathcal{T}})_{\mathfrak{D}} - (A^{\mathfrak{D}}\nabla^{\mathfrak{D}} u^{\mathcal{T}}\cdot\vec{n}, \gamma^{\mathcal{T}}(u^{\mathcal{T}}))_{\partial\Omega}\\
&= \sum_{\mathcal{D}\in\mathfrak{D}} m_{\mathcal{D}}(A_{\mathcal{D}}\nabla^{\mathcal{D}} u^{\mathcal{T}}, \nabla^{\mathcal{D}} u^{\mathcal{T}}) - \sum_{\mathcal{D}\in\mathfrak{D}_{\Gamma}} m_\sigma \gamma^{\mathcal{D}}(u^{\mathcal{T}})(A_{\mathcal{D}}\nabla^{\mathcal{D}} u^{\mathcal{T}}, \vec{n}_{\sigma\mathcal{L}}).
\end{aligned}$$

Combining the last two equalities, we get

$$0 = \sum_{\mathcal{D}\in\mathfrak{D}} m_{\mathcal{D}}(A_{\mathcal{D}}\nabla^{\mathcal{D}}u^{\mathcal{T}}, \nabla^{\mathcal{D}}u^{\mathcal{T}}) + \frac{\lambda}{4}\sum_{\mathcal{D}\in\mathfrak{D}_\Gamma} M_\sigma(u_{\mathcal{K}^*} - u_{\mathcal{L}^*})^2 - \sum_{\mathcal{D}\in\mathfrak{D}_{i,\Gamma}} m_\sigma \gamma^{\mathcal{D}}(u^{\mathcal{T}})(A_{\mathcal{D}}\nabla^{\mathcal{D}}u^{\mathcal{T}}, \vec{n}_{\sigma\mathcal{L}}). \quad (3.6)$$

Using Definition 2.2 of the trace operator $\gamma^{\mathcal{D}}$ and (3.4d), the last term becomes

$$\begin{aligned} &-\sum_{\mathcal{D}\in\mathfrak{D}_\Gamma} m_\sigma \gamma^{\mathcal{D}}(u^{\mathcal{T}})(A_{\mathcal{D}}\nabla^{\mathcal{D}}u^{\mathcal{T}}, \vec{n}_{\sigma\mathcal{L}}) \\ &= -\sum_{\mathcal{D}\in\mathfrak{D}_\Gamma} m_\sigma \left(\frac{m_{\mathcal{K}^*,\mathcal{L}}}{m_\sigma}\gamma_{\mathcal{K}^*,\mathcal{L}}(u^{\mathcal{T}}) + \frac{m_{\mathcal{L}^*,\mathcal{L}}}{m_\sigma}\gamma_{\mathcal{L}^*,\mathcal{L}}(u^{\mathcal{T}})\right)\left(\frac{m_{\mathcal{K}^*,\mathcal{L}}}{m_\sigma}\varphi_{\mathcal{K}^*,\mathcal{L}} + \frac{m_{\mathcal{L}^*,\mathcal{L}}}{m_\sigma}\varphi_{\mathcal{L}^*,\mathcal{L}}\right) \\ &= \sum_{\mathcal{D}\in\mathfrak{D}_\Gamma} m_\sigma \lambda \left(\frac{m_{\mathcal{K}^*,\mathcal{L}}}{m_\sigma}\gamma_{\mathcal{K}^*,\mathcal{L}}(u^{\mathcal{T}}) + \frac{m_{\mathcal{L}^*,\mathcal{L}}}{m_\sigma}\gamma_{\mathcal{L}^*,\mathcal{L}}(u^{\mathcal{T}})\right)^2, \end{aligned}$$

since $\varphi_{\mathcal{K}^*,\mathcal{L}} + \lambda\gamma_{\mathcal{K}^*,\mathcal{L}}(u^{\mathcal{T}}) = 0$ and $\varphi_{\mathcal{L}^*,\mathcal{L}} + \lambda\gamma_{\mathcal{L}^*,\mathcal{L}}(u^{\mathcal{T}}) = 0$. It follows from (3.6) that

$$\begin{aligned} 0 \;=\; & \sum_{\mathcal{D}\in\mathfrak{D}} m_{\mathcal{D}}(A_{\mathcal{D}}\nabla^{\mathcal{D}}u^{\mathcal{T}}, \nabla^{\mathcal{D}}u^{\mathcal{T}}) + \frac{\lambda}{4}\sum_{\mathcal{D}\in\mathfrak{D}_\Gamma} M_\sigma(u_{\mathcal{K}^*} - u_{\mathcal{L}^*})^2 \\ & + \sum_{\mathcal{D}\in\mathfrak{D}_\Gamma} m_\sigma \lambda \left(\frac{m_{\mathcal{K}^*,\mathcal{L}}}{m_\sigma}\gamma_{\mathcal{K}^*,\mathcal{L}}(u^{\mathcal{T}}) + \frac{m_{\mathcal{L}^*,\mathcal{L}}}{m_\sigma}\gamma_{\mathcal{L}^*,\mathcal{L}}(u^{\mathcal{T}})\right)^2. \end{aligned}$$

Since all the terms above are non-negative, we deduce that:

$$0 = \sum_{\mathcal{D}\in\mathfrak{D}} m_{\mathcal{D}}(A_{\mathcal{D}}\nabla^{\mathcal{D}}u^{\mathcal{T}}, \nabla^{\mathcal{D}}u^{\mathcal{T}}).$$

Finally, $A_{\mathcal{D}}$ being definite positive for any $\mathcal{D} \in \mathfrak{D}$, the above equality leads to $\forall\, \mathcal{D} \in \mathfrak{D},\ \nabla^{\mathcal{D}}u^{\mathcal{T}} = 0$. Hence there exists two constants c_0 and c_1 so that :

$$\begin{aligned} \forall\, \mathcal{K} \in (\mathfrak{M} \cup \partial\mathfrak{M}), \quad & u_{\mathcal{K}} = c_0, \\ \forall\, \mathcal{K}^* \in (\mathfrak{M}^* \cup \partial\mathfrak{M}^*), \quad & u_{\mathcal{K}^*} = c_1, \end{aligned}$$

and since $u^{\mathcal{T}}$ satisfies (3.5), we deduce $c_0 = c_1 = 0$ and finally $u^{\mathcal{T}} = 0$. As $\varphi_{\mathcal{K}^*,\mathcal{L}} + \lambda\gamma_{\mathcal{K}^*,\mathcal{L}}(u^{\mathcal{T}}) = 0$ and $\varphi_{\mathcal{L}^*,\mathcal{L}} + \lambda\gamma_{\mathcal{L}^*,\mathcal{L}}(u^{\mathcal{T}}) = 0$, we obtain that $\varphi_{\mathcal{K}^*,\mathcal{L}} = 0$, and $\varphi_{\mathcal{L}^*,\mathcal{L}} = 0$, therefore $U^{\mathcal{T}} = 0$. □

4. Non-overlapping Schwarz algorithm

Consider a domain Ω split into several non-overlapping subdomains Ω_i. The Schwarz algorithm introduced by Lions (see [7],[8],[13]) for the Laplace problem with homogeneous Dirichlet boundary condition consists, instead of solving the problem in Ω, to solve the Laplace equation successively on each subdomains with homogeneous Dirichlet boundary condition on $\partial\Omega_i \cap \partial\Omega$ and with Fourier boundary condition on the interface $\partial\Omega_i \cap \partial\Omega_j$ if $j \neq i$.

We only consider here the case where Ω_1, Ω_2 are two connected subdomains such that $\Omega = \Omega_1 \cup \Omega_2 \cup \Gamma$, Γ being the interface between the two subdomains $\Gamma = \overline{\Omega_1} \cap \overline{\Omega_2}$ and we assume that Γ is connected and that $\Gamma \cap \partial\Omega \neq \emptyset$. These assumptions are not mandatory but let us simplify the presentation a little.

4.1 *Compatible meshes. Composite mesh*

For each subdomain Ω_i, we consider a m-DDFV mesh $\mathcal{T}_i = (\mathfrak{M}_i, \mathfrak{M}_i^* \cup \partial\mathfrak{M}_i^*)$ and the associated diamond mesh $\mathfrak{D}_i$. We note $\mathfrak{D}_{i,\Gamma} = \{\mathcal{D} \in \mathfrak{D}_i,\ \mathcal{D} \cap \Gamma \neq \emptyset\}$. We will assume that the two meshes are compatible in the following sense.

DEFINITION 4.1 *We say that $\mathcal{T}_1$ and $\mathcal{T}_2$ are compatible, if the following two conditions hold:*

1. *The two meshes have the same vertices on Γ : $X_1^* \cap \Gamma = X_2^* \cap \Gamma$. This implies in particular that the two meshes have the same degenerate control volumes on Γ, that is $\partial\mathfrak{M}_{1,\Gamma} = \partial\mathfrak{M}_{2,\Gamma}$.*

2. *The center $x_{\mathcal{L}}$ of a degenerate interface control volume $\mathcal{L} = [x_{\mathcal{K}^*}, x_{\mathcal{L}^*}] \in \partial\mathfrak{M}_{1,\Gamma} = \partial\mathfrak{M}_{2,\Gamma}$ is the intersection of $(x_{\mathcal{K}^*}, x_{\mathcal{L}^*})$ and $(x_{\mathcal{K}_1}, x_{\mathcal{K}_2})$, where $\mathcal{K}_1 \in \mathfrak{M}_1$ and $\mathcal{K}_2 \in \mathfrak{M}_2$ are the two primal control volumes such that $\mathcal{L} \subset \partial\mathcal{K}_1$ and $\mathcal{L} \subset \partial\mathcal{K}_2$.*

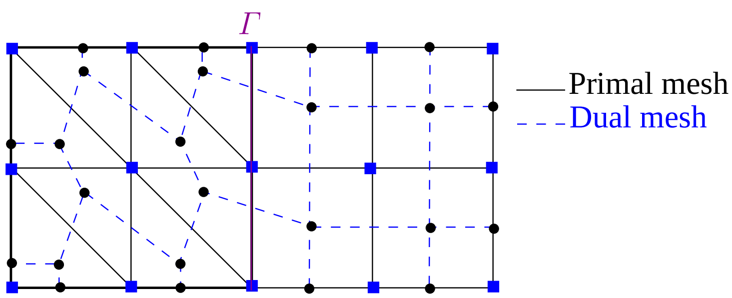

FIG. 4.1. A DDFV mesh $\mathcal{T}$ of the whole domain Ω.

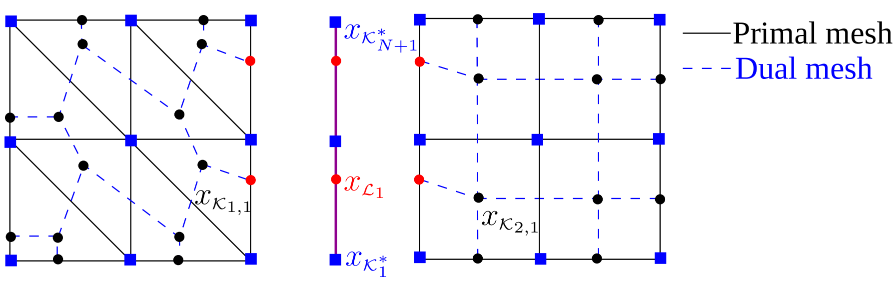

FIG. 4.2. The compatible meshes $\mathcal{T}_1$ and $\mathcal{T}_2$ corresponding to the DDFV mesh $\mathcal{T}$ of the whole domain Ω of Figure 4.1.

REMARK 4.1 *In practice, the two compatibility conditions do not represent important constraints on the meshes under consideration. Indeed, we will usually encounter two opposite situations:*

1. *We are given a DDFV mesh $\mathcal{T}$ of the whole domain Ω (see Figure 4.1) such that any primal control volume $\mathcal{K} \in \mathfrak{M}$ is such that either $\mathcal{K} \subset \Omega_1$ or $\mathcal{K} \subset \Omega_2$. In that case, the construction of*

the two compatible meshes $\mathcal{T}_i$ only amounts to split into pieces the dual control volumes crossing the interface Γ (see Figure 4.2).

2. *We are given* a priori *independent DDFV meshes $\mathcal{T}_i$ for both subdomains Ω_i (see Figure 4.3). In that case, we only have to add some vertices on Γ, ensuring that $\partial\mathfrak{M}_{1,\Gamma} = \partial\mathfrak{M}_{2,\Gamma}$ and then to split the interface dual control volumes in $\partial\mathfrak{M}_{i,\Gamma}$ into pieces in order to take these new vertices into account. The centers $x_{\mathcal{L}}$ of the degenerate interface control volumes are then defined following the second item in Definition 4.1 (see Figure 4.4). Notice that this modification of the meshes do not increase significantly the number of degrees of freedom in the problem.*

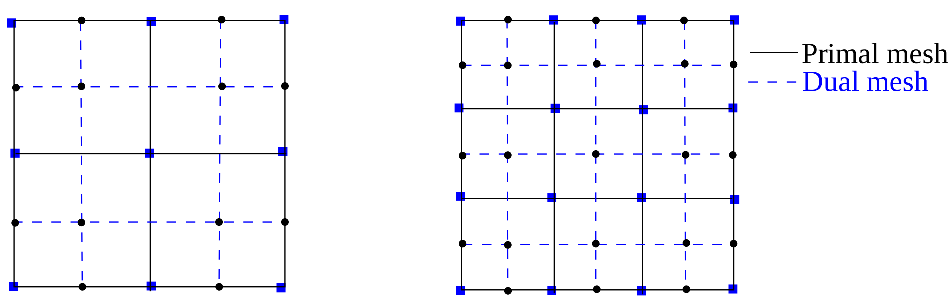

FIG. 4.3. Two independent DDFV meshes $\mathcal{T}_1,\ \mathcal{T}_2$ for both subdomains Ω_i.

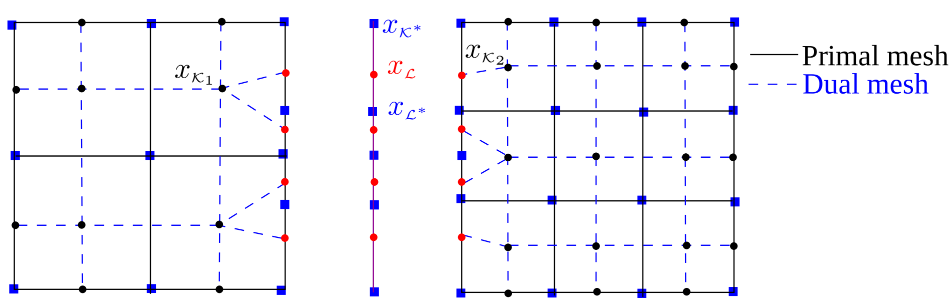

FIG. 4.4. The compatible meshes corresponding to two independent DDFV meshes $\mathcal{T}_1,\ \mathcal{T}_2$ of Figure 4.3 .

For two given compatible meshes $\mathcal{T}_1$ and $\mathcal{T}_2$, we denote by $N+1$ the number of vertices in the two meshes belonging to the interface Γ (these are the same for the two meshes thanks to the compatibility conditions).

For the sake of clarity of some computations below we need to sort and number these $N+1$ vertices $x_{\mathcal{K}_1^*}, \cdots, x_{\mathcal{K}_{N+1}^*}$, in such a way that $[x_{\mathcal{K}_k^*}, x_{\mathcal{K}_{k+1}^*}] \in \partial\mathfrak{M}_{i,\Gamma} = \partial\mathfrak{M}_{j,\Gamma}$ and such that $\{x_{\mathcal{K}_1^*}, x_{\mathcal{K}_{N+1}^*}\} = \Gamma \cap \partial\Omega$ (see Figure 4.5). We do the same with the N centers $x_{\mathcal{L}} \in \Gamma$ which are then sorted and numbered as follows : $x_{\mathcal{L}_1}, \cdots, x_{\mathcal{L}_N}$ with $\mathcal{L}_k = [x_{\mathcal{K}_k^*}, x_{\mathcal{K}_{k+1}^*}]$.

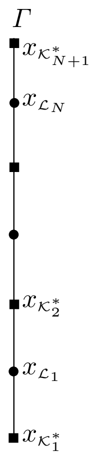

FIG. 4.5. Notations.

Given two compatible meshes $\mathcal{T}_1$ and $\mathcal{T}_2$ in the sense of Definition 4.1, a composite DDFV mesh $\mathcal{T} = (\mathfrak{M}, \mathfrak{M}^* \cup \partial\mathfrak{M}^*)$ can be built on the whole domain Ω. Notice that in the case 1 of Remark 4.1, this composite mesh $\mathcal{T}$ is already available by construction (see Figure 4.1). In other cases, the composite primal mesh is simply given by $\mathfrak{M} = \mathfrak{M}_1 \cup \mathfrak{M}_2$. Then, we need to join corresponding interface dual control volumes in the two meshes. To this end, we introduce the set

$$\mathfrak{M}^*_\Gamma = \{\mathcal{K}^* = \overset{\circ}{\widehat{\overline{\mathcal{K}^*_1} \cup \overline{\mathcal{K}^*_2}}},\ \mathcal{K}^*_1 \in \partial\mathfrak{M}^*_{1,\Gamma},\ \mathcal{K}^*_2 \in \partial\mathfrak{M}^*_{2,\Gamma},\ \text{such that } x_{\mathcal{K}^*_1} = x_{\mathcal{K}^*_2}\},$$

so that the composite interior dual mesh $\mathfrak{M}^*$ is then defined by $\mathfrak{M}^* = \mathfrak{M}^*_1 \cup \mathfrak{M}^*_2 \cup \mathfrak{M}^*_\Gamma$. Finally, the boundary dual cells are the ones in $\partial\mathfrak{M}^* = \partial\mathfrak{M}^*_{1,D} \cup \partial\mathfrak{M}^*_{2,D}$ (see Figure 4.6). Notice that the degenerate interface control volumes $\mathcal{L} \in \partial\mathfrak{M}_{1,\Gamma} = \partial\mathfrak{M}_{2,\Gamma}$ are no more present in the composite mesh. In particular, the corresponding unknowns in the following schemes have no natural corresponding unknown for the m-DDFV scheme on the mesh $\mathcal{T}$.

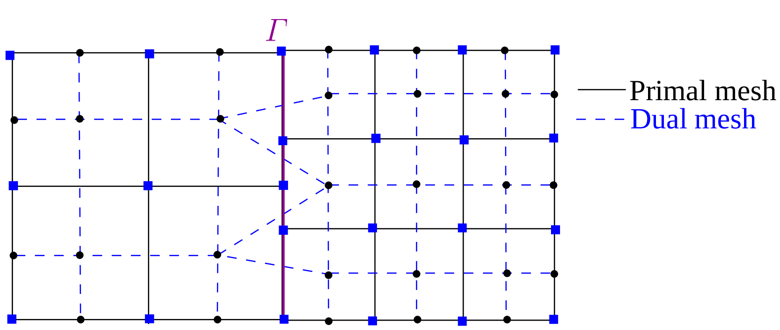

FIG. 4.6. The composite mesh $\mathcal{T}$ corresponding to the 2 compatible meshes of Figure 4.4.

4.2 *Presentation of the iterative domain decomposition solver*

The idea of the domain decomposition method is to use the scheme (3.1) on each of the two subdomains in order to build an iterative Schwarz method which will converge to the solution of the standard m-DDFV scheme on the whole domain Ω for the mesh $\mathcal{T}$. More precisely, we propose the following algorithm

- For any $i \in \{1,2\}$, choose any $g_0^{\mathcal{T}_i} \in \Phi_\Gamma^{\mathcal{T}_i}$.
- For any $n \geqslant 0$, and any $i, j \in \{1,2\}$, $j \neq i$:
  - Calculate $U_{n+1}^{\mathcal{T}_i} = (u_{n+1}^{\mathcal{T}_i}, \phi_{n+1}^{\mathcal{T}_i}) \in \mathbb{R}^{\mathcal{T}_i} \times \Phi_\Gamma^{\mathcal{T}_i}$ solution to
  $$\mathcal{L}_{\Omega_i,\Gamma}^{\mathcal{T}_i}(u_{n+1}^{\mathcal{T}_i}, \phi_{n+1}^{\mathcal{T}_i}, f^{\mathcal{T}_i}, h^{\mathcal{T}_i}, g_n^{\mathcal{T}_j}) = 0. \tag{4.1}$$
  - Calculate $g_{n+1}^{\mathcal{T}_i}$ by
  $$\forall\, [x_{\mathcal{K}^*} x_{\mathcal{L}}] \in \partial\mathfrak{A}_\Gamma, \quad g_{i,\mathcal{K}^*,\mathcal{L}}^{n+1} = -\varphi_{i,\mathcal{K}^*,\mathcal{L}}^{n+1} + \lambda \frac{u_{i,\mathcal{K}^*}^{n+1} + u_{i,\mathcal{L}}^{n+1}}{2}. \tag{4.2}$$

Remark that equality (4.2) is exactly the discrete counterpart of the Lions interface conditions, at the continuous level [13]:

$$(A(x)\nabla u_i^{n+1}, \vec{n}_i) + \lambda u_i^{n+1} = -(A(x)\nabla u_j^n, \vec{n}_j) + \lambda u_j^n,$$

where $\vec{n}_i$ is oriented from Ω_i to Ω_j and $\vec{n}_j = -\vec{n}_i$. That is

$$-(A(x)\nabla u_i^{n+1}, \vec{n}_i) = \lambda u_i^{n+1} - g_j^n,$$

with $g_j^n = -(A(x)\nabla u_j^n, \vec{n}_j) + \lambda u_j^n$. Indeed, $\varphi_{i,\mathcal{K}^*,\mathcal{L}}^{n+1}$ $\left(\text{resp. } \dfrac{u_{i,\mathcal{K}^*}^{n+1} + u_{i,\mathcal{L}}^{n+1}}{2}\right)$ is supposed to approach $(A(x)\nabla u_i^{n+1}, \vec{n}_i)$ $\big(\text{resp. } u_i^{n+1}\big)$.

Using Theorem 3.2, we have the following well-posedness result.

PROPOSITION 4.1 *The initial data $g_0^{\mathcal{T}_i}$ being given, Algorithm* (4.1)-(4.2) *defines a unique sequence $(U_n^{\mathcal{T}_i})_n$ in $\mathbb{R}^{\mathcal{T}_i} \times \Phi_\Gamma^{\mathcal{T}_i}$, for $i = 1, 2$.*

We want now to show that this sequence converges towards the solution of the scheme on the complete domain Ω, for the composite mesh $\mathcal{T}$.

4.3 *Preliminary construction*

The first step in the analysis is to show that the solution of the m-DDFV scheme on the whole domain Ω with homogeneous Dirichlet condition can be written as a possible limit of the sequence $(U_n^{\mathcal{T}_i})_n$, $i \in \{1,2\}$ obtained by the Schwarz algorithm. The precise result is the following:

THEOREM 4.1 (LINK WITH THE M-DDFV SCHEME) *Let $u^{\mathcal{T}}$ be the solution of the m-DDFV scheme with homogeneous Dirichlet condition (that is system* (3.1) *with $\Gamma = \emptyset$) on the whole domain Ω associated with the composite mesh $\mathcal{T}$ built upon $\mathcal{T}_1$ and $\mathcal{T}_2$. For each $i \in \{1,2\}$, there exists $(u^{\mathcal{T}_i}, \phi^{\mathcal{T}_i}, g^{\mathcal{T}_i}) \in \mathbb{R}^{\mathcal{T}_i} \times \Phi_\Gamma^{\mathcal{T}_i} \times \Phi_\Gamma^{\mathcal{T}_i}$ such that*

$$\mathcal{L}_{\Omega_i,\Gamma}^{\mathcal{T}_i}(u^{\mathcal{T}_i}, \phi^{\mathcal{T}_i}, f^{\mathcal{T}_i}, h^{\mathcal{T}_i}, g^{\mathcal{T}_i}) = 0, \tag{4.3}$$

for $i = 1, 2$ *, we have*

$$\begin{cases} u_{i,\mathcal{K}} = u_{\mathcal{K}}, & \text{for } \mathcal{K} \in \mathfrak{M}_i \cup \partial\mathfrak{M}_{i,D}, \\ u_{i,\mathcal{K}^*} = u_{\mathcal{K}^*}, & \text{for } \mathcal{K}^* \in \mathfrak{M}_i^* \cup \partial\mathfrak{M}_i^*, \end{cases} \tag{4.4}$$

and

$$\sum_{k=1}^{N} \left(\varphi_{i,\mathcal{K}_k^*,\mathcal{L}_k} - \varphi_{i,\mathcal{K}_{k+1}^*,\mathcal{L}_k} \right) = 0 \quad \text{for } i = 1,\ 2. \tag{4.5}$$

Proof.

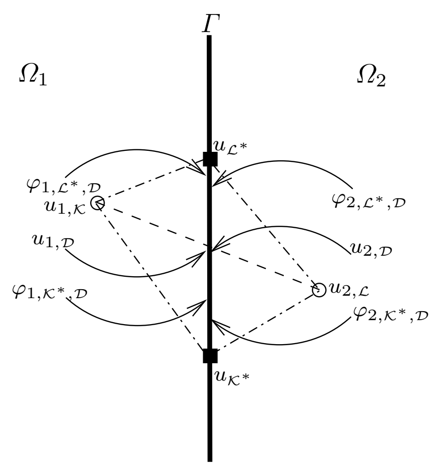

FIG. 4.7. Notations in a diamond cell intersecting the interface Γ.

Equations (4.4) define all the values of $u^{\mathcal{T}_i}$, except the values on the degenerate primal control volumes inside Γ, on both sides of the interface, therefore it remains to define the values of $u_{i,\mathcal{D}}$ and $\varphi_{i,\mathcal{K}^*,\mathcal{D}}$ on the interface Γ.

STEP 1 - COMPUTATION OF THE INTERFACE VALUES. Let us consider $\mathcal{D} \in \mathfrak{D}$ which intersects Γ. Such a diamond cell writes $\overline{\mathcal{D}} = \overline{\mathcal{D}^1} \cup \overline{\mathcal{D}^2}$ where $\mathcal{D}^1 \in \mathfrak{D}_1$, $\mathcal{D}^2 \in \mathfrak{D}_2$. We denote by $\mathcal{K} \in \mathfrak{M}_1$, $\mathcal{L} \in \mathfrak{M}_2$, the primal control volumes such that $\mathcal{D}^1 \subset \mathcal{K}$ and $\mathcal{D}^2 \subset \mathcal{L}$ respectively. We first require the equality $u_{1,\mathcal{D}} = u_{2,\mathcal{D}}$. Then the common value $u_{\mathcal{D}}$ of $u_{1,\mathcal{D}} = u_{2,\mathcal{D}}$ is determined by requiring the local conservativity of normal fluxes:

$$\left(A_{\mathcal{K}} \nabla^{\mathcal{D}^1} u^{\mathcal{T}_1}, \vec{n}_{\sigma\mathcal{K}} \right) = \left(A_{\mathcal{L}} \nabla^{\mathcal{D}^2} u^{\mathcal{T}_2}, \vec{n}_{\sigma\mathcal{K}} \right). \tag{4.6}$$

Using the discrete gradient definition (2.3), this reads

$$\begin{aligned} &\left(\frac{1}{2m_{\mathcal{D}_\mathcal{K}}} \left[(u_{\mathcal{D}} - u_{1,\mathcal{K}}) m_\sigma A_{\mathcal{K}} \vec{n}_{\sigma\mathcal{K}} + (u_{1,\mathcal{L}^*} - u_{1,\mathcal{K}^*}) m_{\sigma_\mathcal{K}} A_{\mathcal{K}} \vec{n}_{\sigma^*\mathcal{K}^*} \right], \vec{n}_{\sigma\mathcal{K}} \right) \\ &= \left(\frac{1}{2m_{\mathcal{D}_\mathcal{L}}} \left[-(u_{\mathcal{D}} - u_{2,\mathcal{L}}) m_\sigma A_{\mathcal{L}} \vec{n}_{\sigma\mathcal{K}} + (u_{2,\mathcal{L}^*} - u_{2,\mathcal{K}^*}) m_{\sigma_\mathcal{L}} A_{\mathcal{L}} \vec{n}_{\sigma^*\mathcal{K}^*} \right], \vec{n}_{\sigma\mathcal{K}} \right) \\ &= \left(\frac{1}{2m_{\mathcal{D}_\mathcal{L}}} \left[-(u_{\mathcal{D}} - u_{2,\mathcal{L}}) m_\sigma A_{\mathcal{L}} \vec{n}_{\sigma\mathcal{K}} + (u_{\mathcal{L}^*} - u_{\mathcal{K}^*}) m_{\sigma_\mathcal{L}} A_{\mathcal{L}} \vec{n}_{\sigma^*\mathcal{K}^*} \right], \vec{n}_{\sigma\mathcal{K}} \right). \end{aligned}$$

As we have $2m_{\mathcal{D}_\mathcal{K}} = \sin\alpha_\mathcal{D} m_\sigma m_{\sigma_\mathcal{K}}$ and $2m_{\mathcal{D}_\mathcal{L}} = \sin\alpha_\mathcal{D} m_\sigma m_{\sigma_\mathcal{L}}$, we obtain

$$u_\mathcal{D}\left(\left(\frac{A_\mathcal{K}}{m_{\sigma_\mathcal{K}}}+\frac{A_\mathcal{L}}{m_{\sigma_\mathcal{L}}}\right)\vec{n}_{\sigma\mathcal{K}},\vec{n}_{\sigma\mathcal{K}}\right) = u_{1,\mathcal{K}}\frac{(A_\mathcal{K}\vec{n}_{\sigma\mathcal{K}},\vec{n}_{\sigma\mathcal{K}})}{m_{\sigma_\mathcal{K}}} + u_{2,\mathcal{L}}\frac{(A_\mathcal{L}\vec{n}_{\sigma\mathcal{K}},\vec{n}_{\sigma\mathcal{K}})}{m_{\sigma_\mathcal{L}}} + \frac{u_{\mathcal{L}^*}-u_{\mathcal{K}^*}}{m_\sigma}\left((A_\mathcal{L}-A_\mathcal{K})\,\vec{n}_{\sigma^*\mathcal{K}^*},\vec{n}_{\sigma\mathcal{K}}\right),$$

and we finally find the following value for $u_\mathcal{D}$:

$$u_\mathcal{D} = \frac{m_{\sigma_\mathcal{K}} m_{\sigma_\mathcal{L}}}{\left((A_\mathcal{K} m_{\sigma_\mathcal{L}} + A_\mathcal{L} m_{\sigma_\mathcal{K}})\,\vec{n}_{\sigma\mathcal{K}},\vec{n}_{\sigma\mathcal{K}}\right)}\Bigg[u_{1,\mathcal{K}}\frac{(A_\mathcal{K}\vec{n}_{\sigma\mathcal{K}},\vec{n}_{\sigma\mathcal{K}})}{m_{\sigma_\mathcal{K}}} + u_{2,\mathcal{L}}\frac{(A_\mathcal{L}\vec{n}_{\sigma\mathcal{K}},\vec{n}_{\sigma\mathcal{K}})}{m_{\sigma_\mathcal{L}}} + \frac{u_{\mathcal{L}^*}-u_{\mathcal{K}^*}}{m_\sigma}\left((A_\mathcal{L}-A_\mathcal{K})\,\vec{n}_{\sigma^*\mathcal{K}^*},\vec{n}_{\sigma\mathcal{K}}\right)\Bigg]. \tag{4.7}$$

STEP 2 - CONSEQUENCES ON THE NUMERICAL FLUXES. The value of $u_\mathcal{D}$ given in (4.7) implies, with our particular choice of $A^\mathfrak{D}$ in (3.2a)-(3.2c), that the following equalities hold:

$$\left(A_\mathcal{D}\nabla^\mathcal{D} u^\mathcal{T},\vec{n}_{\sigma\mathcal{K}}\right) = \left(A_{\mathcal{D}^1}\nabla^{\mathcal{D}^1} u^{\mathcal{T}_1},\vec{n}_{\sigma\mathcal{K}}\right) = \left(A_{\mathcal{D}^2}\nabla^{\mathcal{D}^2} u^{\mathcal{T}_2},\vec{n}_{\sigma\mathcal{K}}\right), \tag{4.8}$$

$$m_{\sigma^*}\left(A_\mathcal{D}\nabla^\mathcal{D} u^\mathcal{T},\vec{n}_{\sigma^*\mathcal{K}^*}\right) = m_{\sigma_\mathcal{K}}\left(A_\mathcal{K}\nabla^{\mathcal{D}^1} u^{\mathcal{T}_1},\vec{n}_{\sigma^*\mathcal{K}^*}\right) + m_{\sigma_\mathcal{L}}\left(A_\mathcal{L}\nabla^{\mathcal{D}^2} u^{\mathcal{T}_2},\vec{n}_{\sigma^*\mathcal{K}^*}\right). \tag{4.9}$$

Equality (4.8) comes from the definition (2.3) of the discrete gradient, the definition (3.2a) and (3.2c) of $A^\mathfrak{D}$ and the value of $u_\mathcal{D}$ obtained in (4.7).

Let us now give a detailed proof for (4.9). Using the definition (2.3) of the discrete gradient, we get

$$\begin{aligned}
&m_{\sigma^*}\left(A_\mathcal{D}\nabla^\mathcal{D} u^\mathcal{T},\vec{n}_{\sigma^*\mathcal{K}^*}\right) - m_{\sigma_\mathcal{K}}\left(A_\mathcal{K}\nabla^{\mathcal{D}^1} u^{\mathcal{T}_1},\vec{n}_{\sigma^*\mathcal{K}^*}\right) - m_{\sigma_\mathcal{L}}\left(A_\mathcal{L}\nabla^{\mathcal{D}^2} u^{\mathcal{T}_2},\vec{n}_{\sigma^*\mathcal{K}^*}\right)\\
&= \frac{u_{2,\mathcal{L}}-u_{1,\mathcal{K}}}{2m_\mathcal{D}} m_{\sigma^*} m_\sigma (A_\mathcal{D}\vec{n}_{\sigma\mathcal{K}},\vec{n}_{\sigma^*\mathcal{K}^*}) + \frac{(u_{\mathcal{L}^*}-u_{\mathcal{K}^*})}{2m_\mathcal{D}} m_{\sigma^*} m_{\sigma^*} (A_\mathcal{D}\vec{n}_{\sigma^*\mathcal{K}^*},\vec{n}_{\sigma^*\mathcal{K}^*})\\
&- \frac{u_\mathcal{D}-u_{1,\mathcal{K}}}{2m_{\mathcal{D}_\mathcal{K}}} m_{\sigma_\mathcal{K}} m_\sigma (A_\mathcal{K}\vec{n}_{\sigma\mathcal{K}},\vec{n}_{\sigma^*\mathcal{K}^*}) - \frac{(u_{\mathcal{L}^*}-u_{\mathcal{K}^*})}{2m_{\mathcal{D}_\mathcal{K}}} m_{\sigma_\mathcal{K}} m_{\sigma_\mathcal{K}} (A_\mathcal{K}\vec{n}_{\sigma^*\mathcal{K}^*},\vec{n}_{\sigma^*\mathcal{K}^*})\\
&+ \frac{u_\mathcal{D}-u_{2,\mathcal{L}}}{2m_{\mathcal{D}_\mathcal{L}}} m_{\sigma_\mathcal{L}} m_\sigma (A_\mathcal{L}\vec{n}_{\sigma\mathcal{K}},\vec{n}_{\sigma^*\mathcal{K}^*}) - \frac{(u_{\mathcal{L}^*}-u_{\mathcal{K}^*})}{2m_{\mathcal{D}_\mathcal{L}}} m_{\sigma_\mathcal{L}} m_{\sigma_\mathcal{L}} (A_\mathcal{L}\vec{n}_{\sigma^*\mathcal{K}^*},\vec{n}_{\sigma^*\mathcal{K}^*}).
\end{aligned}$$

Using formula (4.7), we can reorganize all the terms as follows

$$\begin{aligned}
&m_{\sigma^*}\left(A_\mathcal{D}\nabla^\mathcal{D} u^\mathcal{T},\vec{n}_{\sigma^*\mathcal{K}^*}\right) - m_{\sigma_\mathcal{K}}\left(A_\mathcal{K}\nabla^{\mathcal{D}^1} u^{\mathcal{T}_1},\vec{n}_{\sigma^*\mathcal{K}^*}\right) - m_{\sigma_\mathcal{L}}\left(A_\mathcal{L}\nabla^{\mathcal{D}^2} u^{\mathcal{T}_2},\vec{n}_{\sigma^*\mathcal{K}^*}\right)\\
&= u_{1,\mathcal{K}} T_\mathcal{K} + u_{2,\mathcal{L}} T_\mathcal{L} + (u_{\mathcal{K}^*}-u_{\mathcal{L}^*}) T^*,
\end{aligned} \tag{4.10}$$

where

$$T_\mathcal{K} = \frac{1}{\sin\alpha_\mathcal{D}}\Bigg[(A_\mathcal{K}\vec{n}_{\sigma\mathcal{K}},\vec{n}_{\sigma^*\mathcal{K}^*}) - (A_\mathcal{D}\vec{n}_{\sigma\mathcal{K}},\vec{n}_{\sigma^*\mathcal{K}^*}) + ((A_\mathcal{L}-A_\mathcal{K})\vec{n}_{\sigma\mathcal{K}},\vec{n}_{\sigma^*\mathcal{K}^*}) m_{\sigma_\mathcal{L}} \frac{(A_\mathcal{K}\vec{n}_{\sigma\mathcal{K}},\vec{n}_{\sigma\mathcal{K}})}{\left((A_\mathcal{K} m_{\sigma_\mathcal{L}} + A_\mathcal{L} m_{\sigma_\mathcal{K}})\,\vec{n}_{\sigma\mathcal{K}},\vec{n}_{\sigma\mathcal{K}}\right)}\Bigg],$$

$$T_{\mathcal{L}} = \frac{1}{\sin\alpha_{\mathcal{D}}}\Bigg[(A_{\mathcal{D}}\vec{n}_{\sigma\mathcal{K}},\vec{n}_{\sigma^*\mathcal{K}^*}) - (A_{\mathcal{L}}\vec{n}_{\sigma\mathcal{K}},\vec{n}_{\sigma^*\mathcal{K}^*}) + ((A_{\mathcal{L}}-A_{\mathcal{K}})\vec{n}_{\sigma\mathcal{K}},\vec{n}_{\sigma^*\mathcal{K}^*})m_{\sigma\mathcal{K}}\frac{(A_{\mathcal{L}}\vec{n}_{\sigma\mathcal{K}},\vec{n}_{\sigma\mathcal{K}})}{((A_{\mathcal{K}}m_{\sigma_{\mathcal{L}}}+A_{\mathcal{L}}m_{\sigma_{\mathcal{K}}})\,\vec{n}_{\sigma\mathcal{K}},\vec{n}_{\sigma\mathcal{K}})}\Bigg],$$

and

$$T^* = \frac{1}{\sin\alpha_{\mathcal{D}}}\Bigg[\frac{m_{\sigma^*}}{m_\sigma}(A_{\mathcal{D}}\vec{n}_{\sigma^*\mathcal{K}^*},\vec{n}_{\sigma^*\mathcal{K}^*}) - \frac{m_{\sigma_{\mathcal{K}}}}{m_\sigma}(A_{\mathcal{K}}\vec{n}_{\sigma^*\mathcal{K}^*},\vec{n}_{\sigma^*\mathcal{K}^*}) - \frac{m_{\sigma_{\mathcal{L}}}}{m_\sigma}(A_{\mathcal{L}}\vec{n}_{\sigma^*\mathcal{K}^*},\vec{n}_{\sigma^*\mathcal{K}^*}) + \frac{m_{\sigma_{\mathcal{K}}}m_{\sigma_{\mathcal{L}}}\,((A_{\mathcal{L}}-A_{\mathcal{K}})\,\vec{n}_{\sigma^*\mathcal{K}^*},\vec{n}_{\sigma\mathcal{K}})^2}{m_\sigma\,((A_{\mathcal{K}}m_{\sigma_{\mathcal{L}}}+A_{\mathcal{L}}m_{\sigma_{\mathcal{K}}})\,\vec{n}_{\sigma\mathcal{K}},\vec{n}_{\sigma\mathcal{K}})}\Bigg].$$

Using the definition (3.2c) of $(A_{\mathcal{D}}\vec{n}_{\sigma\mathcal{K}},\vec{n}_{\sigma^*\mathcal{K}^*})$, $T_{\mathcal{K}}$ becomes

$$T_{\mathcal{K}} = \Big[m_{\sigma_{\mathcal{L}}}(A_{\mathcal{K}}\vec{n}_{\sigma\mathcal{K}},\vec{n}_{\sigma^*\mathcal{K}^*})(A_{\mathcal{K}}\vec{n}_{\sigma\mathcal{K}},\vec{n}_{\sigma\mathcal{K}}) + m_{\sigma_{\mathcal{K}}}(A_{\mathcal{K}}\vec{n}_{\sigma\mathcal{K}},\vec{n}_{\sigma^*\mathcal{K}^*})(A_{\mathcal{L}}\vec{n}_{\sigma\mathcal{K}},\vec{n}_{\sigma\mathcal{K}}) - m_{\sigma_{\mathcal{L}}}(A_{\mathcal{K}}\vec{n}_{\sigma\mathcal{K}},\vec{n}_{\sigma\mathcal{K}})(A_{\mathcal{L}}\vec{n}_{\sigma\mathcal{K}},\vec{n}_{\sigma^*\mathcal{K}^*}) - m_{\sigma_{\mathcal{K}}}(A_{\mathcal{K}}\vec{n}_{\sigma\mathcal{K}},\vec{n}_{\sigma^*\mathcal{K}^*})(A_{\mathcal{L}}\vec{n}_{\sigma\mathcal{K}},\vec{n}_{\sigma\mathcal{K}}) + m_{\sigma_{\mathcal{L}}}((A_{\mathcal{L}}-A_{\mathcal{K}})\vec{n}_{\sigma\mathcal{K}},\vec{n}_{\sigma^*\mathcal{K}^*})(A_{\mathcal{K}}\vec{n}_{\sigma\mathcal{K}},\vec{n}_{\sigma\mathcal{K}})\Big]\Big/\Big[\sin\alpha_{\mathcal{D}}\,((A_{\mathcal{K}}m_{\sigma_{\mathcal{L}}}+A_{\mathcal{L}}m_{\sigma_{\mathcal{K}}})\,\vec{n}_{\sigma\mathcal{K}},\vec{n}_{\sigma\mathcal{K}})\Big],$$

which gives $T_{\mathcal{K}} = 0$. Similarly, by using the definition (3.2c) of $(A_{\mathcal{D}}\vec{n}_{\sigma\mathcal{K}},\vec{n}_{\sigma^*\mathcal{K}^*})$, we get that $T_{\mathcal{L}}$ is also equal to zero. Using the definition (3.2b) of $(A_{\mathcal{D}}\vec{n}_{\sigma^*\mathcal{K}^*},\vec{n}_{\sigma^*\mathcal{K}^*})$, T^* becomes

$$\begin{aligned} T^* \;=\; \frac{1}{m_\sigma \sin\alpha_{\mathcal{D}}}\Bigg[& m_{\sigma_{\mathcal{L}}}(A_{\mathcal{L}}\vec{n}_{\sigma^*\mathcal{K}^*},\vec{n}_{\sigma^*\mathcal{K}^*}) + m_{\sigma_{\mathcal{K}}}(A_{\mathcal{K}}\vec{n}_{\sigma^*\mathcal{K}^*},\vec{n}_{\sigma^*\mathcal{K}^*}) \\ & - m_{\sigma_{\mathcal{K}}}m_{\sigma_{\mathcal{L}}}\frac{((A_{\mathcal{K}}-A_{\mathcal{L}})\vec{n}_{\sigma\mathcal{K}},\vec{n}_{\sigma^*\mathcal{K}^*})^2}{((A_{\mathcal{K}}m_{\sigma_{\mathcal{L}}}+A_{\mathcal{L}}m_{\sigma_{\mathcal{K}}})\,\vec{n}_{\sigma\mathcal{K}},\vec{n}_{\sigma\mathcal{K}})} \\ & - m_{\sigma_{\mathcal{K}}}(A_{\mathcal{K}}\vec{n}_{\sigma^*\mathcal{K}^*},\vec{n}_{\sigma^*\mathcal{K}^*}) - m_{\sigma_{\mathcal{L}}}(A_{\mathcal{L}}\vec{n}_{\sigma^*\mathcal{K}^*},\vec{n}_{\sigma^*\mathcal{K}^*}) \\ & + m_{\sigma_{\mathcal{K}}}m_{\sigma_{\mathcal{L}}}\frac{((A_{\mathcal{K}}-A_{\mathcal{L}})\vec{n}_{\sigma\mathcal{K}},\vec{n}_{\sigma^*\mathcal{K}^*})^2}{((A_{\mathcal{K}}m_{\sigma_{\mathcal{L}}}+A_{\mathcal{L}}m_{\sigma_{\mathcal{K}}})\,\vec{n}_{\sigma\mathcal{K}},\vec{n}_{\sigma\mathcal{K}})}\Bigg], \end{aligned}$$

and we see that $T^* = 0$. Hence (4.10) leads to (4.9).

STEP 3 - COMPUTATION OF THE FLUX UNKNOWNS. In the sequel, all mathematical objects associated to a subdomain Ω_i will be marked with the index i as follows

- $\mathcal{D}_k^i$ is the k^{th} diamond belonging to $\mathfrak{D}_{i,\Gamma}$ with respect to the numerotation introduced in Figure 4.5. In particular, $\mathcal{D}_k^i \subset \Omega_i$.
- $\mathcal{K}_{i,k}^*$ is the k^{th} dual cell on Γ belonging to $\partial\mathfrak{M}_{i,\Gamma}^*$, and then $\mathcal{K}_{i,k}^* \subset \Omega_i$.

We have $2N$ unknowns $\varphi_{i,\mathcal{K}^*,\mathcal{L}}$ and only $2N-1$ equations, that is the reason why we impose the normalisation condition (4.5) in order to uniquely define the flux unknowns $\varphi_{i,\mathcal{K}^*,\mathcal{L}}$. Let us study separately what takes place on each sub-domain. We have to solve the following linear system for the sub-domain Ω_1

$$\underbrace{\begin{pmatrix} d_1 & d_2 & & & \\ & d_2 & d_3 & & \\ & & \ddots & \ddots & \\ & & & d_{2N-1} & d_{2N} \\ 1 & -1 & \cdots & 1 & -1 \end{pmatrix}}_{=B} \underbrace{\begin{pmatrix} \varphi_{1,\mathcal{K}_1^*,\mathcal{L}_1} \\ \varphi_{1,\mathcal{K}_2^*,\mathcal{L}_1} \\ \vdots \\ \varphi_{1,\mathcal{K}_N^*,\mathcal{L}_N} \\ \varphi_{1,\mathcal{K}_{N+1}^*,\mathcal{L}_N} \end{pmatrix}}_{=\Phi_1} = \begin{pmatrix} m_{\sigma_1}\left(A_{\mathcal{D}_1^1}\nabla^{\mathcal{D}_1^1}u^{\mathcal{T}_1}, \vec{n}_{\sigma\mathcal{L}_1}\right) \\ -m_{\mathcal{K}_{1,2}^*}f_{\mathcal{K}_{1,2}^*} - \sum_{\mathcal{D}\in\mathfrak{D}_{\mathcal{K}_{1,2}^*}} m_{\sigma^*}\left(A_{\mathcal{D}}\nabla^{\mathcal{D}}u^{\mathcal{T}_1}, \vec{n}_{\sigma^*\mathcal{K}_2^*}\right) \\ \vdots \\ m_{\sigma_N}\left(A_{\mathcal{D}_N^1}\nabla^{\mathcal{D}_N^1}u^{\mathcal{T}_1}, \vec{n}_{\sigma\mathcal{L}_N}\right) \\ 0 \end{pmatrix}, \tag{4.11}$$

using the notations $d_{2k-1} = m_{\mathcal{K}_k^*,\mathcal{L}_k}$ and $d_{2k} = m_{\mathcal{K}_{k+1}^*,\mathcal{L}_k}$ for any $k = 1, \cdots, N$. We easily see that B is invertible, so that there exists a unique vector Φ_1 solving (4.11).

Let us now look at the sub-domain Ω_2. We just define $\Phi_2 = -\Phi_1$ and we have to prove that Φ_2 satisfies the following system on Ω_2:

$$B\Phi_2 = \begin{pmatrix} m_{\sigma_1}\left(A_{\mathcal{D}_1^2}\nabla^{\mathcal{D}_1^2}u^{\mathcal{T}_2}, \vec{n}_{\sigma\mathcal{L}_1}\right) \\ -m_{\mathcal{K}_{2,2}^*}f_{\mathcal{K}_{2,2}^*} - \sum_{\mathcal{D}\in\mathfrak{D}_{\mathcal{K}_{2,2}^*}} m_{\sigma^*}\left(A_{\mathcal{D}}\nabla^{\mathcal{D}}u^{\mathcal{T}_2}, \vec{n}_{\sigma^*\mathcal{K}_2^*}\right) \\ \vdots \\ m_{\sigma_N}\left(A_{\mathcal{D}_N^2}\nabla^{\mathcal{D}_N^2}u^{\mathcal{T}_2}, \vec{n}_{\sigma\mathcal{L}_N}\right) \\ 0 \end{pmatrix}, \tag{4.12}$$

with the convention that $\vec{n}_{\sigma\mathcal{L}_k}$ is the outward unit normal to Ω_1 on σ, for all $k = 1, \cdots, N$. Using the fact that $\Phi_2 = -\Phi_1$ and equation (4.11), we have for all $k = 1, \cdots, N$

$$\begin{aligned} m_{\mathcal{K}_k^*,\mathcal{L}_k}\varphi_{2,\mathcal{K}_k^*,\mathcal{L}_k} + m_{\mathcal{K}_{k+1}^*,\mathcal{L}_k}\varphi_{2,\mathcal{K}_{k+1}^*,\mathcal{L}_k} &= -m_{\mathcal{K}_k^*,\mathcal{L}_k}\varphi_{1,\mathcal{K}_k^*,\mathcal{L}_k} - m_{\mathcal{K}_{k+1}^*,\mathcal{L}_k}\varphi_{1,\mathcal{K}_{k+1}^*,\mathcal{L}_k} \\ &= -m_{\sigma_k}\left(A_{\mathcal{D}_k^1}\nabla^{\mathcal{D}_k^1}u^{\mathcal{T}_1}, \vec{n}_{\sigma\mathcal{L}_k}\right). \end{aligned}$$

Using the local conservativity equation (4.6), we obtain for all $k = 1, \cdots, N$

$$m_{\mathcal{K}_k^*,\mathcal{L}_k}\varphi_{2,\mathcal{K}_k^*,\mathcal{L}_k} + m_{\mathcal{K}_{k+1}^*,\mathcal{L}_k}\varphi_{2,\mathcal{K}_{k+1}^*,\mathcal{L}_k} = -m_{\sigma_k}\left(A_{\mathcal{D}_k^2}\nabla^{\mathcal{D}_k^2}u^{\mathcal{T}_2}, \vec{n}_{\sigma\mathcal{L}_k}\right).$$

Let $k \in \{2, \cdots, N\}$. On the one hand, by definition of $\varphi_{1,\mathcal{K}^*,\mathcal{L}}$ we have:

$$-\sum_{\mathcal{D}\in\mathfrak{D}_{\mathcal{K}_{1,k}^*}} m_{\sigma^*}\left(A_{\mathcal{D}}\nabla^{\mathcal{D}}u^{\mathcal{T}_1}, \vec{n}_{\sigma^*\mathcal{K}_k^*}\right) - m_{\mathcal{K}_k^*,\mathcal{L}_k}\varphi_{1,\mathcal{K}_k^*,\mathcal{L}_k} - m_{\mathcal{K}_k^*,\mathcal{L}_{k-1}}\varphi_{1,\mathcal{K}_k^*,\mathcal{L}_{k-1}} = m_{\mathcal{K}_{1,k}^*}f_{\mathcal{K}_{1,k}^*}.$$

On the other hand, there exists a unique $\mathcal{K}_k^* \in \mathfrak{M}^*$, and we have $\overline{\mathcal{K}_k^*} = \overline{\mathcal{K}_{1,k}^*} \cup \overline{\mathcal{K}_{2,k}^*}$, with $\mathcal{K}_{2,k}^* \in \mathfrak{M}_2^*$, see Figure 4.8.

Since, $u^{\mathcal{T}}$ solves the m-DDFV scheme on the mesh $\mathcal{T}$, we have in particular the following equation

$$-\sum_{\mathcal{D}\in\mathfrak{D}_{\mathcal{K}_k^*}} m_{\sigma^*}\left(A_{\mathcal{D}}\nabla^{\mathcal{D}}u^{\mathcal{T}}, \vec{n}_{\sigma^*\mathcal{K}_k^*}\right) = m_{\mathcal{K}_k^*}f_{\mathcal{K}_k^*}.$$

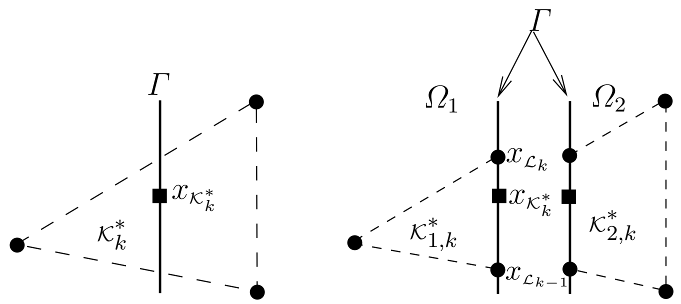

FIG. 4.8. Decomposition of $\mathcal{K}_k^*$ into the two dual cells of the subdomains.

Using equality (4.9) and the fact that $\Phi_2 = -\Phi_1$, it follows that

$$\begin{aligned}
& -\sum_{\mathcal{D}\in\mathfrak{D}_{\mathcal{K}^*_{2,k}}} m_{\sigma^*}\left(A_{\mathcal{D}}\nabla^{\mathcal{D}}u^{\mathcal{T}_2}, \vec{n}_{\sigma^*\mathcal{K}_k^*}\right) - m_{\mathcal{K}_k^*,\mathcal{L}_k}\varphi_{2,\mathcal{K}_k^*,\mathcal{L}_k} - m_{\mathcal{K}_k^*,\mathcal{L}_{k-1}}\varphi_{2,\mathcal{K}_k^*,\mathcal{L}_{k-1}} \\
= & -\sum_{\mathcal{D}\in\mathfrak{D}_{\mathcal{K}^*_{k}}} m_{\sigma^*}\left(A_{\mathcal{D}}\nabla^{\mathcal{D}}u^{\mathcal{T}}, \vec{n}_{\sigma^*\mathcal{K}_k^*}\right) + \sum_{\mathcal{D}\in\mathfrak{D}_{\mathcal{K}^*_{1,k}}} m_{\sigma^*}\left(A_{\mathcal{D}}\nabla^{\mathcal{D}}u^{\mathcal{T}_1}, \vec{n}_{\sigma^*\mathcal{K}_k^*}\right) \\
& + m_{\mathcal{K}_k^*,\mathcal{L}_k}\varphi_{1,\mathcal{K}_k^*,\mathcal{L}_k} + m_{\mathcal{K}_k^*,\mathcal{L}_{k-1}}\varphi_{1,\mathcal{K}_k^*,\mathcal{L}_{k-1}} \\
= & \; m_{\mathcal{K}_k^*}f_{\mathcal{K}_k^*} - m_{\mathcal{K}_{1,k}^*}f_{\mathcal{K}_{1,k}^*} = \int_{\mathcal{K}_k^*} f(x)\,dx - \int_{\mathcal{K}_{1,k}^*} f(x)\,dx \\
= & \int_{\mathcal{K}_{2,k}^*} f(x)\,dx = m_{\mathcal{K}_{2,k}^*}f_{\mathcal{K}_{2,k}^*},
\end{aligned}$$

which exactly gives (4.12).

STEP 4 - CONCLUDING THE PROOF. It remains to define $g^{\mathcal{T}_i}$, for $i = 1, 2$, as follows:

$$g_{i,\mathcal{K}^*,\mathcal{L}} = -\varphi_{i,\mathcal{K}^*,\mathcal{L}} + \lambda\frac{u_{i,\mathcal{K}^*} + u_{i,\mathcal{L}}}{2}. \tag{4.13}$$

Collecting all the previous results, we see that we get a solution to

$$\mathcal{L}^{\mathcal{T}_i}_{\Omega_i,\Gamma}(u^{\mathcal{T}_i}, \phi^{\mathcal{T}_i}, f^{\mathcal{T}_i}, h^{\mathcal{T}_i}, g^{\mathcal{T}_j}) = 0$$

for $i = 1, 2$, $j \neq i$ and satisfying furthermore the condition (4.5).

□

REMARK 4.2 (BARYCENTRIC DUAL MESH) *If we use the* barycentric dual mesh *and the notations of Figure 3.1, we have a new definition of the common value $u_{\mathcal{D}}$ as follows*

$$\begin{aligned}
u_{\mathcal{D}} = \frac{m_{\sigma\mathcal{K}}m_{\sigma\mathcal{L}}}{((A_{\mathcal{K}}m_{\sigma\mathcal{L}} + A_{\mathcal{L}}m_{\sigma\mathcal{K}})\,\vec{n}_{\sigma\mathcal{K}}, \vec{n}_{\sigma\mathcal{K}})}\Bigg[& u_{1,\mathcal{K}}\frac{(A_{\mathcal{K}}\vec{n}_{\sigma\mathcal{K}}, \vec{n}_{\sigma\mathcal{K}})}{m_{\sigma\mathcal{K}}} + u_{2,\mathcal{L}}\frac{(A_{\mathcal{L}}\vec{n}_{\sigma\mathcal{K}}, \vec{n}_{\sigma\mathcal{K}})}{m_{\sigma\mathcal{L}}} \\
& + \frac{u_{\mathcal{L}^*} - u_{\mathcal{K}^*}}{m_\sigma}\left(A_{\mathcal{L}}\frac{m_{\sigma_2^*}}{m_{\sigma\mathcal{L}}}\vec{n}_{\sigma_2^*\mathcal{K}^*} - A_{\mathcal{K}}\frac{m_{\sigma_1^*}}{m_{\sigma\mathcal{K}}}\vec{n}_{\sigma_1^*\mathcal{K}^*}, \vec{n}_{\sigma\mathcal{K}}\right)\Bigg].
\end{aligned} \tag{4.7-bis}$$

Using the corresponding modified definition of $A_{\mathcal{D}}$ (3.2a), (3.2b-bis) *and* (3.2c-bis), *and the value of* $u_{\mathcal{D}}$ *given in* (4.7-bis), *the equality* (4.8) *still holds whereas the equality* (4.9) *naturally becomes:*

$$m_{\sigma^*}\left(A_{\mathcal{D}}\nabla^{\mathcal{D}}u^{\mathcal{T}},\vec{n}_{\sigma^*\mathcal{K}^*}\right)=m_{\sigma_1^*}\left(A_{\mathcal{K}}\nabla^{\mathcal{D}^1}u^{\mathcal{T}_1},\vec{n}_{\sigma_1^*\mathcal{K}^*}\right)+m_{\sigma_2^*}\left(A_{\mathcal{L}}\nabla^{\mathcal{D}^2}u^{\mathcal{T}_2},\vec{n}_{\sigma_2^*\mathcal{K}^*}\right). \qquad \text{(4.9-bis)}$$

Hence, the proof of Theorem 4.1 can be easily adapted to this case. Notice in particular that the choice of the barycentric dual mesh implies that the entries d_i *of matrix* B *in* (4.11) *are always positive and then* B *is always invertible. Note also that the convergence proof given in the following section can be easily adapted to this case.*

4.4 *Convergence analysis of the iterative method*

Let us state the discrete version of the Poincaré inequality which is proved in [2, Lemma 3.3].

LEMMA 4.1 (DISCRETE POINCARÉ INEQUALITY) *Let T be a DDFV mesh of* Ω*. There exists* $C>0$*, depending only on the diameter of* Ω *and on* $\mathrm{reg}(\mathcal{T})$ *such that for any* $u^{\mathcal{T}}\in\mathbb{R}^{\mathcal{T}}$ *and any* $g\in H^{\frac{1}{2}}(\partial\Omega)$*, we have*

$$||u^{\mathcal{T}}||_2\leqslant||u^{\mathfrak{M}}||_2+||u^{\mathfrak{M}^*}||_2\leqslant C\left(||\nabla^{\mathfrak{D}}u^{\mathcal{T}}||_2+||g||_{H^{\frac{1}{2}}(\partial\Omega)}\right).$$

The number $C>0$ in this result depends on the number $\mathrm{reg}(\mathcal{T})$ which is a measure of the regularity of the mesh. Since we are working in this paper with a fixed mesh $\mathcal{T}$, its precise definition is not needed and we refer to [2] for the details. Let us only point out that $\mathrm{reg}(\mathcal{T})$ essentially measures how flat the diamond cells are and how large is the ratio between the diameter of a primal cell (resp. dual cell) and the diameter of a diamond cell as soon as they intersect.

It is now possible, as in [4] for the classical five point finite volume scheme, to prove the main result of this paper, that is the convergence of the Schwarz iterative method to the solution of the m-DDFV scheme.

THEOREM 4.2 (CONVERGENCE OF THE SCHWARZ ALGORITHM) *For any* $g_0^{\mathcal{T}_i}\in\Phi_{\Gamma}^{\mathcal{T}_i}$, $i\in\{1,2\}$, *the solution* $(u_n^{\mathcal{T}_i})_{i=1,2}$ *of the algorithm* (4.1)-(4.2) *converges to the solution* $u^{\mathcal{T}}$ *of the m-DDFV scheme with homogeneous Dirichlet condition (that is system* (3.1) *with* $\Gamma=\emptyset$*) when* $n\longrightarrow\infty$.

Moreover, if we assume that $g_0^{\mathcal{T}_i}$ *is chosen in such a way that*

$$\sum_{k=1}^{N}\left(g^0_{i,\mathcal{K}_k^*,\mathcal{L}_k}-g^0_{i,\mathcal{K}_{k+1}^*,\mathcal{L}_k}\right)=\frac{\lambda}{2}\left(h_{\mathcal{K}_1^*}-h_{\mathcal{K}_{N+1}^*}\right),\ \ i=\{1,2\}, \qquad (4.14)$$

then, the flux unknowns $\varphi^{n+1}_{i,\mathcal{K}^*,\mathcal{L}}$ *given by algorithm* (4.1)-(4.2) *also converge to the flux approximations* $\varphi^{\mathcal{T}}_{i,\mathcal{K}^*,\mathcal{L}}$ *of the scheme* (4.3) *when* $n\longrightarrow\infty$ *that is to say that the solution* U^{n+1} *of the algorithm* (4.1)-(4.2) *converge to the solution* $U^{\mathcal{T}}$ *of the scheme* (4.3) *when* $n\longrightarrow\infty$.

Note that the values of $u_n^{\mathcal{T}_1}$ and $u_n^{\mathcal{T}_2}$ corresponding to the same points on the interface Γ may not coincide, in general, but they both converge to the same value when n goes to infinity.

Proof.

For $i\in\{1,2\}$, we define the errors on each sub-domain at iteration number n as follows

$$e_i^n=u_i^{\mathcal{T}}-u_i^n,\ \ \psi^n_{i,\mathcal{K}^*,\mathcal{L}}=\varphi_{i,\mathcal{K}^*,\mathcal{L}}-\varphi^n_{i,\mathcal{K}^*,\mathcal{L}},\ \ \bar{g}^n_{i,\mathcal{K}^*,\mathcal{L}}=g_{i,\mathcal{K}^*,\mathcal{L}}-g^n_{i,\mathcal{K}^*,\mathcal{L}}.$$

These error terms satisfy the following system : for $i = 1, 2$ and $j \neq i$.

$$-\text{div}^{\mathcal{K}}\left(A^{\mathfrak{D}}\nabla^{\mathfrak{D}}e_i^{n+1}\right) = 0, \ \forall \, \mathcal{K} \in \mathfrak{M}_i, \tag{4.15a}$$

$$-\text{div}^{\mathcal{K}^*}\left(A^{\mathfrak{D}}\nabla^{\mathfrak{D}}e_i^{n+1}\right) = 0, \ \forall \, \mathcal{K}^* \in \mathfrak{M}_i^*, \tag{4.15b}$$

$$-\sum_{\mathcal{D}\in\mathfrak{D}_{\mathcal{K}_k^*}} m_{\sigma^*}\left(A_{\mathcal{D}}\nabla^{\mathcal{D}}e_i^{n+1}, \vec{n}_{\sigma^*\mathcal{K}_k^*}\right) - m_{\mathcal{K}_k^*,\mathcal{L}_k}\psi_{i,\mathcal{K}_k^*,\mathcal{L}_k}^{n+1} - m_{\mathcal{K}_k^*,\mathcal{L}_{k-1}}\psi_{i,\mathcal{K}_k^*,\mathcal{L}_{k-1}}^{n+1} = 0, \ \forall \, k \in \{2, \cdots, N\}, \tag{4.15c}$$

$$\frac{m_{\mathcal{K}_k^*,\mathcal{L}_k}}{m_\sigma}\psi_{i,\mathcal{K}_k^*,\mathcal{L}_k}^{n+1} + \frac{m_{\mathcal{K}_{k+1}^*,\mathcal{L}_k}}{m_\sigma}\psi_{i,\mathcal{K}_{k+1}^*,\mathcal{L}_k}^{n+1} - \left(A_{\mathcal{D}}\nabla^{\mathcal{D}}e_i^{n+1}, \vec{n}_{\sigma\mathcal{L}_k}\right) = 0, \ \forall \, k \in \{1, \cdots, N\}, \tag{4.15d}$$

$$e_{i,\mathcal{K}}^{n+1} = 0, \ \forall \, \mathcal{K} \in \partial\mathfrak{M}_D, \qquad e_{i,\mathcal{K}^*}^{n+1} = 0, \ \forall \, \mathcal{K}^* \in \partial\mathfrak{M}_D^*, \tag{4.15e}$$

$$\psi_{i,\mathcal{K}_k^*,\mathcal{L}_k}^{n+1} + \lambda\gamma_{\mathcal{K}_k^*,\mathcal{L}_k}\left(e_i^{n+1}\right) = \bar{g}_{j,\mathcal{K}_k^*,\mathcal{L}_k}^n \ \ \forall \, k \in \{1, \cdots, N\}, \tag{4.15f}$$

$$\psi_{i,\mathcal{K}_{k+1}^*,\mathcal{L}_k}^{n+1} + \lambda\gamma_{\mathcal{K}_{k+1}^*,\mathcal{L}_k}\left(e_i^{n+1}\right) = \bar{g}_{j,\mathcal{K}_{k+1}^*,\mathcal{L}_k}^n \ \ \forall \, k \in \{1, \cdots, N\}, \tag{4.15g}$$

with

$$\bar{g}_{j,\mathcal{K}^*,\mathcal{L}}^n = -\psi_{j,\mathcal{K}^*,\mathcal{L}}^n + \lambda\gamma_{\mathcal{K}^*,\mathcal{L}}\left(e_j^n\right) \quad \forall [x_{\mathcal{K}^*}x_{\mathcal{L}}] \in \partial\mathfrak{A}_\Gamma. \tag{4.16}$$

STEP 1. Let us define $I_i^{n+1} = -[\![\text{div}^{\mathcal{T}}(A^{\mathfrak{D}}\nabla^{\mathfrak{D}}e_i^{n+1}), e_i^{n+1}]\!]_{\mathcal{T}_i}$. Using Lemma 3.1, we have :

$$I_i^{n+1} = -\frac{\lambda}{4}\sum_{k=1}^{N} M_{\sigma_k}\left(e_{i,\mathcal{K}_k^*}^{n+1} - e_{i,\mathcal{K}_{k+1}^*}^{n+1}\right)^2 - \frac{1}{2}\sum_{k=2}^{N} e_{i,\mathcal{K}_k^*}^{n+1} M_{\sigma_k}\left(\bar{g}_{j,\mathcal{K}_{k+1}^*,\mathcal{L}_k}^n - \bar{g}_{j,\mathcal{K}_k^*,\mathcal{L}_k}^n\right) - \frac{1}{2}\sum_{k=2}^{N} e_{i,\mathcal{K}_k^*}^{n+1} M_{\sigma_{k-1}}\left(\bar{g}_{j,\mathcal{K}_{k-1}^*,\mathcal{L}_{k-1}}^n - \bar{g}_{j,\mathcal{K}_k^*,\mathcal{L}_{k-1}}^n\right),$$

where we recall that $M_{\sigma_k} = \frac{m_{\mathcal{K}_k^*,\mathcal{L}_k}\, m_{\mathcal{K}_{k+1}^*,\mathcal{L}_k}}{m_{\sigma_k}}$. Equation (4.16) for the Fourier data error term and the definition (2.2) of $\gamma_{\mathcal{K}^*,\mathcal{L}}$ lead to

$$\begin{aligned} I_i^{n+1} \quad = \quad & -\frac{\lambda}{4}\sum_{k=1}^{N} M_{\sigma_k}\left(e_{i,\mathcal{K}_k^*}^{n+1} - e_{i,\mathcal{K}_{k+1}^*}^{n+1}\right)^2 \\ & -\frac{1}{2}\sum_{k=2}^{N} e_{i,\mathcal{K}_k^*}^{n+1} M_{\sigma_k}\left(-\left(\psi_{j,\mathcal{K}_{k+1}^*,\mathcal{L}_k}^n - \psi_{j,\mathcal{K}_k^*,\mathcal{L}_k}^n\right)\right) \\ & -\frac{1}{2}\sum_{k=2}^{N} e_{i,\mathcal{K}_k^*}^{n+1} M_{\sigma_{k-1}}\left(-\left(\psi_{j,\mathcal{K}_{k-1}^*,\mathcal{L}_{k-1}}^n - \psi_{j,\mathcal{K}_k^*,\mathcal{L}_{k-1}}^n\right)\right) \\ & -\frac{\lambda}{4}\sum_{k=2}^{N} e_{i,\mathcal{K}_k^*}^{n+1} M_{\sigma_k}\left(e_{j,\mathcal{K}_{k+1}^*}^n - e_{j,\mathcal{K}_k^*}^n\right) - \frac{\lambda}{4}\sum_{k=2}^{N} e_{i,\mathcal{K}_k^*}^{n+1} M_{\sigma_{k-1}}\left(e_{j,\mathcal{K}_{k-1}^*}^n - e_{j,\mathcal{K}_k^*}^n\right). \end{aligned}$$

As a consequence, by gathering all the similar terms, we get

$$
\begin{aligned}
I_i^{n+1} =& -\frac{\lambda}{4}\sum_{k=1}^{N} M_{\sigma_k}\left(e^{n+1}_{i,\mathcal{K}^*_k}-e^{n+1}_{i,\mathcal{K}^*_{k+1}}\right)^2 \\
& -\frac{1}{2}\sum_{k=1}^{N} M_{\sigma_k}\left(-\left(\psi^n_{j,\mathcal{K}^*_{k+1},\mathcal{L}_k}-\psi^n_{j,\mathcal{K}^*_k,\mathcal{L}_k}\right)\right)\left(e^{n+1}_{i,\mathcal{K}^*_k}-e^{n+1}_{i,\mathcal{K}^*_{k+1}}\right) \\
& +\frac{\lambda}{4}\sum_{k=2}^{N} M_{\sigma_k}\left(e^{n}_{j,\mathcal{K}^*_{k+1}}-e^{n}_{j,\mathcal{K}^*_k}\right)\left(e^{n+1}_{i,\mathcal{K}^*_{k+1}}-e^{n+1}_{i,\mathcal{K}^*_k}\right).
\end{aligned}
\tag{4.17}
$$

STEP 2 . We can now compute I_i^{n+1} in a different way, by using the discrete Stokes formula (2.5) on the sub-domain Ω_i:

$$
\begin{aligned}
I_i^{n+1} &= (A^{\mathfrak{D}}\nabla^{\mathfrak{D}} e_i^{n+1}, \nabla^{\mathfrak{D}} e_i^{n+1})_{\mathfrak{D}_i} - (\gamma^{\mathfrak{D}_i}(A^{\mathfrak{D}}\nabla^{\mathfrak{D}} e_i^{n+1}\cdot\vec{n}), \gamma^{\mathcal{T}}(e_i^{n+1}))_{\partial\Omega_i} \\
&= \sum_{\mathcal{D}\in\mathfrak{D}_i} m_{\mathcal{D}}(A_{\mathcal{D}}\nabla^{\mathcal{D}} e_i^{n+1}, \nabla^{\mathcal{D}} e_i^{n+1}) - \sum_{\mathcal{D}\in\mathfrak{D}_{i,\Gamma}} m_\sigma \gamma^{\mathcal{D}}(e_i^{n+1})(A_{\mathcal{D}}\nabla^{\mathcal{D}} e_i^{n+1}, \vec{n}_{\sigma\mathcal{L}}).
\end{aligned}
\tag{4.18}
$$

By comparing (4.17) and (4.18), we obtain

$$
\begin{aligned}
0 =& \sum_{\mathcal{D}\in\mathfrak{D}_i} m_{\mathcal{D}}(A_{\mathcal{D}}\nabla^{\mathcal{D}} e_i^{n+1}, \nabla^{\mathcal{D}} e_i^{n+1}) \\
& +\frac{\lambda}{4}\sum_{k=1}^{N} M_{\sigma_k}\left(e^{n+1}_{i,\mathcal{K}^*_k}-e^{n+1}_{i,\mathcal{K}^*_{k+1}}\right)^2 - \frac{\lambda}{4}\sum_{k=2}^{N} M_{\sigma_k}\left(e^{n}_{j,\mathcal{K}^*_{k+1}}-e^{n}_{j,\mathcal{K}^*_k}\right)\left(e^{n+1}_{i,\mathcal{K}^*_{k+1}}-e^{n+1}_{i,\mathcal{K}^*_k}\right) \\
& \underbrace{+\frac{1}{2}\sum_{k=1}^{N} M_{\sigma_k}\left(-\left(\psi^n_{j,\mathcal{K}^*_{k+1},\mathcal{L}_k}-\psi^n_{j,\mathcal{K}^*_k,\mathcal{L}_k}\right)\right)\left(e^{n+1}_{i,\mathcal{K}^*_k}-e^{n+1}_{i,\mathcal{K}^*_{k+1}}\right)}_{=B_1} \\
& \underbrace{-\sum_{\mathcal{D}\in\mathfrak{D}_{i,\Gamma}} m_\sigma \gamma^{\mathcal{D}}(e_i^{n+1})(A_{\mathcal{D}}\nabla^{\mathcal{D}} e_i^{n+1}, \vec{n}_{\sigma\mathcal{L}})}_{=B_2}.
\end{aligned}
\tag{4.19}
$$

Equation (4.15d) and Definition (2.2) of the trace operator $\gamma^{\mathcal{D}}$ imply that the term B_2 writes

$$
\begin{aligned}
B_2 = \sum_{k=1}^{N} m_{\sigma_k} \quad & \left(\frac{m_{\mathcal{K}^*_k,\mathcal{L}_k}}{m_{\sigma_k}}\gamma_{\mathcal{K}^*_k,\mathcal{L}_k}(e_i^{n+1}) + \frac{m_{\mathcal{K}^*_{k+1},\mathcal{L}_k}}{m_{\sigma_k}}\gamma_{\mathcal{K}^*_{k+1},\mathcal{L}_k}(e_i^{n+1})\right) \\
& \times\left(\frac{m_{\mathcal{K}^*_k,\mathcal{L}_k}}{m_{\sigma_k}}\psi^{n+1}_{i,\mathcal{K}^*_k,\mathcal{L}_k} + \frac{m_{\mathcal{K}^*_{k+1},\mathcal{L}_k}}{m_{\sigma_k}}\psi^{n+1}_{i,\mathcal{K}^*_{k+1},\mathcal{L}_k}\right).
\end{aligned}
$$

We now use (4.15f)-(4.15g) and (4.16) to find that

$$
\psi^n_{j,\mathcal{K}^*_{k+1},\mathcal{L}_k}-\psi^n_{j,\mathcal{K}^*_k,\mathcal{L}_k} = \frac{\lambda}{2}\left(e^{n+1}_{i,\mathcal{K}^*_k}-e^{n+1}_{i,\mathcal{K}^*_{k+1}}\right) + \frac{\lambda}{2}\left(e^{n}_{j,\mathcal{K}^*_{k+1}}-e^{n}_{j,\mathcal{K}^*_k}\right) + \psi^{n+1}_{i,\mathcal{K}^*_k,\mathcal{L}_k} - \psi^{n+1}_{i,\mathcal{K}^*_{k+1},\mathcal{L}_k},
$$

in the term B_1, it follows that $\widetilde{B} = B_1 - B_2$ writes:

$$\left.\begin{aligned}\widetilde{B} \quad = \quad & -\frac{\lambda}{4}\sum_{k=1}^{N} M_{\sigma_k}\left(e^{n+1}_{i,\mathcal{K}^*_k} - e^{n+1}_{i,\mathcal{K}^*_{k+1}}\right)^2 \\ & +\frac{\lambda}{4}\sum_{k=1}^{N} M_{\sigma_k}\left(e^{n}_{j,\mathcal{K}^*_k} - e^{n}_{j,\mathcal{K}^*_{k+1}}\right)\left(e^{n+1}_{i,\mathcal{K}^*_k} - e^{n+1}_{i,\mathcal{K}^*_{k+1}}\right) \\ & -\frac{1}{2}\sum_{k=1}^{N} M_{\sigma_k}\left(\psi^{n+1}_{i,\mathcal{K}^*_k,\mathcal{L}_k} - \psi^{n+1}_{i,\mathcal{K}^*_{k+1},\mathcal{L}_k}\right)\left(e^{n+1}_{i,\mathcal{K}^*_k} - e^{n+1}_{i,\mathcal{K}^*_{k+1}}\right) \\ & -\sum_{k=1}^{N} \left(\frac{m_{\mathcal{K}^*_k,\mathcal{L}_k}}{m_{\sigma_k}}\gamma_{\mathcal{K}^*_k,\mathcal{L}_k}(e^{n+1}_i) + \frac{m_{\mathcal{K}^*_{k+1},\mathcal{L}_k}}{m_{\sigma_k}}\gamma_{\mathcal{K}^*_{k+1},\mathcal{L}_k}(e^{n+1}_i)\right) \\ & \qquad \times\left(m_{\mathcal{K}^*_k,\mathcal{L}_k}\psi^{n+1}_{i,\mathcal{K}^*_k,\mathcal{L}_k} + m_{\mathcal{K}^*_{k+1},\mathcal{L}_k}\psi^{n+1}_{i,\mathcal{K}^*_{k+1},\mathcal{L}_k}\right), \end{aligned}\right\} = \widetilde{B}_2$$

and by gathering the two sums in $\widetilde{B}_2$, we easily get

$$\widetilde{B}_2 = -\sum_{k=1}^{N}\left(m_{\mathcal{K}^*_k,\mathcal{L}_k}\psi^{n+1}_{i,\mathcal{K}^*_k,\mathcal{L}_k}\gamma_{\mathcal{K}^*_k,\mathcal{L}_k}(e^{n+1}_i) + m_{\mathcal{K}^*_{k+1},\mathcal{L}_k}\psi^{n+1}_{i,\mathcal{K}^*_{k+1},\mathcal{L}_k}\gamma_{\mathcal{K}^*_{k+1},\mathcal{L}_k}(e^{n+1}_i)\right).$$

Hence, (4.19) becomes

$$\begin{aligned} 0 \quad = \quad & \sum_{\mathcal{D}\in\mathfrak{D}_i} m_{\mathcal{D}}(A_{\mathcal{D}}\nabla^{\mathcal{D}}e^{n+1}_i, \nabla^{\mathcal{D}}e^{n+1}_i) \\ & +\frac{\lambda}{4}\sum_{k=1}^{N} M_{\sigma_k}\left(e^{n+1}_{i,\mathcal{K}^*_k} - e^{n+1}_{i,\mathcal{K}^*_{k+1}}\right)^2 - \frac{\lambda}{4}\sum_{k=2}^{N} M_{\sigma_k}\left(e^{n}_{j,\mathcal{K}^*_{k+1}} - e^{n}_{j,\mathcal{K}^*_k}\right)\left(e^{n+1}_{i,\mathcal{K}^*_{k+1}} - e^{n+1}_{i,\mathcal{K}^*_k}\right) \\ & -\frac{\lambda}{4}\sum_{k=1}^{N} M_{\sigma_k}\left(e^{n+1}_{i,\mathcal{K}^*_k} - e^{n+1}_{i,\mathcal{K}^*_{k+1}}\right)^2 + \frac{\lambda}{4}\sum_{k=1}^{N} M_{\sigma_k}\left(e^{n}_{j,\mathcal{K}^*_k} - e^{n}_{j,\mathcal{K}^*_{k+1}}\right)\left(e^{n+1}_{i,\mathcal{K}^*_k} - e^{n+1}_{i,\mathcal{K}^*_{k+1}}\right) \\ & -\sum_{k=1}^{N}\left[m_{\mathcal{K}^*_k,\mathcal{L}_k}\psi^{n+1}_{i,\mathcal{K}^*_k,\mathcal{L}_k}\gamma_{\mathcal{K}^*_k,\mathcal{L}_k}(e^{n+1}_i) + m_{\mathcal{K}^*_{k+1},\mathcal{L}_k}\psi^{n+1}_{i,\mathcal{K}^*_{k+1},\mathcal{L}_k}\gamma_{\mathcal{K}^*_{k+1},\mathcal{L}_k}(e^{n+1}_i)\right], \end{aligned}$$

and we see that the sum of the second, third, fourth and fifth terms cancels, so that it finally remains

$$\begin{aligned} 0 \quad = \quad & \sum_{\mathcal{D}\in\mathfrak{D}_i} m_{\mathcal{D}}(A_{\mathcal{D}}\nabla^{\mathcal{D}}e^{n+1}_i, \nabla^{\mathcal{D}}e^{n+1}_i) \\ & -\sum_{k=1}^{N}\left[m_{\mathcal{K}^*_k,\mathcal{L}_k}\psi^{n+1}_{i,\mathcal{K}^*_k,\mathcal{L}_k}\gamma_{\mathcal{K}^*_k,\mathcal{L}_k}(e^{n+1}_i) + m_{\mathcal{K}^*_{k+1},\mathcal{L}_k}\psi^{n+1}_{i,\mathcal{K}^*_{k+1},\mathcal{L}_k}\gamma_{\mathcal{K}^*_{k+1},\mathcal{L}_k}(e^{n+1}_i)\right]. \end{aligned}$$

We can do exactly the same computation on the sub-domain Ω_j. Adding the two results, we obtain

$$
\begin{aligned}
0 = &\sum_{\mathcal{D}\in\mathfrak{D}_i} m_{\mathcal{D}}(A_{\mathcal{D}}\nabla^{\mathcal{D}}e_i^{n+1},\nabla^{\mathcal{D}}e_i^{n+1}) + \sum_{\mathcal{D}\in\mathfrak{D}_j} m_{\mathcal{D}}(A_{\mathcal{D}}\nabla^{\mathcal{D}}e_j^{n+1},\nabla^{\mathcal{D}}e_j^{n+1}) \\
&-\sum_{k=1}^{N}\Big[m_{\mathcal{K}_k^*,\mathcal{L}_k}\psi^{n+1}_{i,\mathcal{K}_k^*,\mathcal{L}_k}\gamma_{\mathcal{K}_k^*,\mathcal{L}_k}(e_i^{n+1}) + m_{\mathcal{K}_{k+1}^*,\mathcal{L}_k}\psi^{n+1}_{i,\mathcal{K}_{k+1}^*,\mathcal{L}_k}\gamma_{\mathcal{K}_{k+1}^*,\mathcal{L}_k}(e_i^{n+1})\Big] \\
&-\sum_{k=1}^{N}\Big[m_{\mathcal{K}_k^*,\mathcal{L}_k}\psi^{n+1}_{j,\mathcal{K}_k^*,\mathcal{L}_k}\gamma_{\mathcal{K}_k^*,\mathcal{L}_k}(e_j^{n+1}) + m_{\mathcal{K}_{k+1}^*,\mathcal{L}_k}\psi^{n+1}_{j,\mathcal{K}_{k+1}^*,\mathcal{L}_k}\gamma_{\mathcal{K}_{k+1}^*,\mathcal{L}_k}(e_j^{n+1})\Big].
\end{aligned}
\tag{4.20}
$$

STEP 3. Using the formula

$$
-ab = \frac{1}{4\lambda}\left((a-\lambda b)^2 - (a+\lambda b)^2\right),
$$

and equations (4.15f)-(4.15g) and (4.16), we get that for any $k = 1,\dots,N$:

$$
\begin{aligned}
&-\psi^{n+1}_{i,\mathcal{K}_k^*,\mathcal{L}_k}\gamma_{\mathcal{K}_k^*,\mathcal{L}_k}(e_i^{n+1}) - \psi^{n+1}_{j,\mathcal{K}_k^*,\mathcal{L}_k}\gamma_{\mathcal{K}_k^*,\mathcal{L}_k}(e_j^{n+1}) \\
&= \frac{1}{4\lambda}\left[\left(-\psi^{n+1}_{i,\mathcal{K}_k^*,\mathcal{L}_k} + \lambda\gamma_{\mathcal{K}_k^*,\mathcal{L}_k}(e_i^{n+1})\right)^2 - \left(\underbrace{\psi^{n+1}_{i,\mathcal{K}_k^*,\mathcal{L}_k} + \lambda\gamma_{\mathcal{K}_k^*,\mathcal{L}_k}(e_i^{n+1})}_{=-\psi^n_{j,\mathcal{K}_k^*,\mathcal{L}_k}+\lambda\gamma_{\mathcal{K}_k^*,\mathcal{L}_k}(e_j^n)}\right)^2\right] \\
&+\frac{1}{4\lambda}\left[\left(-\psi^{n+1}_{j,\mathcal{K}_k^*,\mathcal{L}_k} + \lambda\gamma_{\mathcal{K}_k^*,\mathcal{L}_k}(e_j^{n+1})\right)^2 - \left(\underbrace{\psi^{n+1}_{j,\mathcal{K}_k^*,\mathcal{L}_k} + \lambda\gamma_{\mathcal{K}_k^*,\mathcal{L}_k}(e_j^{n+1})}_{=-\psi^n_{i,\mathcal{K}_k^*,\mathcal{L}_k}+\lambda\gamma_{\mathcal{K}_k^*,\mathcal{L}_k}(e_i^n)}\right)^2\right] \\
&= \frac{1}{4\lambda}\left[\left(-\psi^{n+1}_{i,\mathcal{K}_k^*,\mathcal{L}_k} + \lambda\gamma_{\mathcal{K}_k^*,\mathcal{L}_k}(e_i^{n+1})\right)^2 - \left(-\psi^{n}_{i,\mathcal{K}_k^*,\mathcal{L}_k} + \lambda\gamma_{\mathcal{K}_k^*,\mathcal{L}_k}(e_i^{n})\right)^2\right] \\
&+\frac{1}{4\lambda}\left[\left(-\psi^{n+1}_{j,\mathcal{K}_k^*,\mathcal{L}_k} + \lambda\gamma_{\mathcal{K}_k^*,\mathcal{L}_k}(e_j^{n+1})\right)^2 - \left(-\psi^{n}_{j,\mathcal{K}_k^*,\mathcal{L}_k} + \lambda\gamma_{\mathcal{K}_k^*,\mathcal{L}_k}(e_j^{n})\right)^2\right].
\end{aligned}
$$

We can do the same for computing $-\psi^{n+1}_{i,\mathcal{K}_{k+1}^*,\mathcal{L}_k}\gamma_{\mathcal{K}_{k+1}^*,\mathcal{L}_k}(e_i^{n+1}) - \psi^{n+1}_{j,\mathcal{K}_{k+1}^*,\mathcal{L}_k}\gamma_{\mathcal{K}_{k+1}^*,\mathcal{L}_k}(e_j^{n+1})$ with (4.15g) and (4.16). Thus, we find that (4.20) becomes:

$$
\begin{aligned}
0 = &\sum_{\mathcal{D}\in\mathfrak{D}_i} m_{\mathcal{D}}(A_{\mathcal{D}}\nabla^{\mathcal{D}}e_i^{n+1},\nabla^{\mathcal{D}}e_i^{n+1}) + \sum_{\mathcal{D}\in\mathfrak{D}_j} m_{\mathcal{D}}(A_{\mathcal{D}}\nabla^{\mathcal{D}}e_j^{n+1},\nabla^{\mathcal{D}}e_j^{n+1}) \\
&+ \sum_{[x_{\mathcal{K}^*},x_{\mathcal{L}}]\in\partial\mathfrak{A}_\Gamma} \frac{m_{\mathcal{K}^*,\mathcal{L}}}{4\lambda}\left[\left(-\psi^{n+1}_{i,\mathcal{K}^*,\mathcal{L}} + \lambda\gamma_{\mathcal{K}^*,\mathcal{L}}(e_i^{n+1})\right)^2 - \left(-\psi^{n}_{i,\mathcal{K}^*,\mathcal{L}} + \lambda\gamma_{\mathcal{K}^*,\mathcal{L}}(e_i^{n})\right)^2\right] \\
&+ \sum_{[x_{\mathcal{K}^*},x_{\mathcal{L}}]\in\partial\mathfrak{A}_\Gamma} \frac{m_{\mathcal{K}^*,\mathcal{L}}}{4\lambda}\left[\left(-\psi^{n+1}_{j,\mathcal{K}^*,\mathcal{L}} + \lambda\gamma_{\mathcal{K}^*,\mathcal{L}}(e_j^{n+1})\right)^2 - \left(-\psi^{n}_{j,\mathcal{K}^*,\mathcal{L}} + \lambda\gamma_{\mathcal{K}^*,\mathcal{L}}(e_j^{n})\right)^2\right].
\end{aligned}
\tag{4.21}
$$

STEP 4. Let $M \in \mathbb{N}^*$, we sum the equality (4.21) for n varying from 1 to M, and we remark that simplifications occur in the interface terms from iteration n and $n+1$. It follows that

$$\sum_{n=1}^{M}\sum_{\mathcal{D}\in\mathfrak{D}_i} m_{\mathcal{D}}(A_{\mathcal{D}}\nabla^{\mathcal{D}}e_i^{n+1},\nabla^{\mathcal{D}}e_i^{n+1}) + \sum_{n=1}^{M}\sum_{\mathcal{D}\in\mathfrak{D}_j} m_{\mathcal{D}}(A_{\mathcal{D}}\nabla^{\mathcal{D}}e_j^{n+1},\nabla^{\mathcal{D}}e_j^{n+1})$$
$$+ \underbrace{\sum_{[x_{\mathcal{K}^*},x_{\mathcal{L}}]\in\partial\mathfrak{A}_\Gamma} \frac{m_{\mathcal{K}^*,\mathcal{L}}}{4\lambda}\left(-\psi^{M+1}_{i,\mathcal{K}^*,\mathcal{L}}+\lambda\gamma_{\mathcal{K}^*,\mathcal{L}}(e_i^{M+1})\right)^2 + \sum_{[x_{\mathcal{K}^*},x_{\mathcal{L}}]\in\partial\mathfrak{A}_\Gamma} \frac{m_{\mathcal{K}^*,\mathcal{L}}}{4\lambda}\left(-\psi^{M+1}_{j,\mathcal{K}^*,\mathcal{L}}+\lambda\gamma_{\mathcal{K}^*,\mathcal{L}}(e_j^{M+1})\right)^2}_{\geqslant 0}$$
$$= \sum_{[x_{\mathcal{K}^*},x_{\mathcal{L}}]\in\partial\mathfrak{A}_\Gamma} \frac{m_{\mathcal{K}^*,\mathcal{L}}}{4\lambda}\left(-\psi^{1}_{i,\mathcal{K}^*,\mathcal{L}}+\lambda\gamma_{\mathcal{K}^*,\mathcal{L}}(e_i^{1})\right)^2 + \sum_{[x_{\mathcal{K}^*},x_{\mathcal{L}}]\in\partial\mathfrak{A}_\Gamma} \frac{m_{\mathcal{K}^*,\mathcal{L}}}{4\lambda}\left(-\psi^{1}_{j,\mathcal{K}^*,\mathcal{L}}+\lambda\gamma_{\mathcal{K}^*,\mathcal{L}}(e_j^{1})\right)^2,$$

which gives that there exists $C > 0$, independent of n, such that

$$\sum_{n=1}^{M}\sum_{\mathcal{D}\in\mathfrak{D}_i} m_{\mathcal{D}}(A_{\mathcal{D}}\nabla^{\mathcal{D}}e_i^{n+1},\nabla^{\mathcal{D}}e_i^{n+1}) + \sum_{n=1}^{M}\sum_{\mathcal{D}\in\mathfrak{D}_j} m_{\mathcal{D}}(A_{\mathcal{D}}\nabla^{\mathcal{D}}e_j^{n+1},\nabla^{\mathcal{D}}e_j^{n+1}) \quad \leqslant \quad C.$$

Using the coercivity of the matrix-valued map A, we obtain

$$\sum_{n=1}^{M} ||\nabla^{\mathfrak{D}_i}e_i^{n+1}||^2_{\mathfrak{D}_i} + \sum_{n=1}^{M} ||\nabla^{\mathfrak{D}_j}e_j^{n+1}||^2_{\mathfrak{D}_j} \leqslant C_A C.$$

We deduce that the two series $\sum_{n\geqslant 1} ||\nabla^{\mathfrak{D}_i}e_i^{n+1}||^2_{\mathfrak{D}_i}$ and $\sum_{n\geqslant 1} ||\nabla^{\mathfrak{D}_j}e_j^{n+1}||^2_{\mathfrak{D}_j}$ converge and as a result we have that for $i = 1, 2$

$$||\nabla^{\mathfrak{D}_i}e_i^{n+1}||^2_{\mathfrak{D}_i} \underset{n\to+\infty}{\longrightarrow} 0.$$

According to the discrete Poincaré inequality Lemma 4.1, we deduce the convergence of e_i^{n+1} to 0, for $i = 1, 2$, when n goes to ∞.

STEP 5. Let us now prove that the fluxes $\psi^{n+1}_{i,\mathcal{K}^*,\mathcal{L}}$ converge to 0. Using equations (4.15c)-(4.15d), we already have that $\forall\, k \in \{1, \cdots, N\}$:

$$\frac{m_{\mathcal{K}_k^*,\mathcal{L}_k}}{m_\sigma}\psi^{n+1}_{i,\mathcal{K}_k^*,\mathcal{L}_k} + \frac{m_{\mathcal{K}_{k+1}^*,\mathcal{L}_k}}{m_\sigma}\psi^{n+1}_{i,\mathcal{K}_{k+1}^*,\mathcal{L}_k} = \left(A_{\mathcal{D}}\nabla^{\mathcal{D}}e_i^{n+1},\vec{n}_{\sigma\mathcal{L}_k}\right) \underset{n\to+\infty}{\longrightarrow} 0,$$

and $\forall\, k \in \{2, \cdots, N\}$

$$m_{\mathcal{K}_k^*,\mathcal{L}_k}\psi^{n+1}_{i,\mathcal{K}_k^*,\mathcal{L}_k} + m_{\mathcal{K}_k^*,\mathcal{L}_{k-1}}\psi^{n+1}_{i,\mathcal{K}_k^*,\mathcal{L}_{k-1}} = -\sum_{\mathcal{D}\in\mathfrak{D}_{\mathcal{K}_k^*}} m_{\sigma^*}\left(A_{\mathcal{D}}\nabla^{\mathcal{D}}e_i^{n+1},\vec{n}_{\sigma^*\mathcal{K}_k^*}\right) \underset{n\to+\infty}{\longrightarrow} 0.$$

We first prove by induction that for any $n \geqslant 0$, we have

$$\sum_{k=1}^{N}\left(\bar{g}^n_{i,\mathcal{K}_k^*,\mathcal{L}_k} - \bar{g}^n_{i,\mathcal{K}_{k+1}^*,\mathcal{L}_k}\right) = 0. \tag{4.22}$$

For the initialisation, we use the definition of $\bar{g}^0_{i,\mathcal{K}^*,\mathcal{L}}$ to obtain

$$\sum_{k=1}^{N}\left(\bar{g}^0_{i,\mathcal{K}^*_k,\mathcal{L}_k}-\bar{g}^0_{i,\mathcal{K}^*_{k+1},\mathcal{L}_k}\right)=\sum_{k=1}^{N}\left(g_{i,\mathcal{K}^*_k,\mathcal{L}_k}-g_{i,\mathcal{K}^*_{k+1},\mathcal{L}_k}\right)-\sum_{k=1}^{N}\left(g^0_{i,\mathcal{K}^*_k,\mathcal{L}_k}-g^0_{i,\mathcal{K}^*_{k+1},\mathcal{L}_k}\right).$$

Using (4.13), then (4.4) and (3.1e), we have

$$\begin{aligned}\sum_{k=1}^{N}\left(g_{i,\mathcal{K}^*_k,\mathcal{L}_k}-g_{i,\mathcal{K}^*_{k+1},\mathcal{L}_k}\right)&=-\sum_{k=1}^{N}\left(\varphi_{i,\mathcal{K}^*_k,\mathcal{L}_k}-\varphi_{i,\mathcal{K}^*_{k+1},\mathcal{L}_k}\right)+\frac{\lambda}{2}\sum_{k=1}^{N}\left(u_{i,\mathcal{K}^*_k}-u_{i,\mathcal{K}^*_{k+1}}\right)\\&=-\sum_{k=1}^{N}\left(\varphi_{i,\mathcal{K}^*_k,\mathcal{L}_k}-\varphi_{i,\mathcal{K}^*_{k+1},\mathcal{L}_k}\right)+\frac{\lambda}{2}\left(h_{\mathcal{K}^*_1}-h_{\mathcal{K}^*_{N+1}}\right),\end{aligned}$$

and then, by using (4.5), we finally have

$$\sum_{k=1}^{N}\left(g_{i,\mathcal{K}^*_k,\mathcal{L}_k}-g_{i,\mathcal{K}^*_{k+1},\mathcal{L}_k}\right)=\frac{\lambda}{2}\left(h_{\mathcal{K}^*_1}-h_{\mathcal{K}^*_{N+1}}\right).$$

This implies by using (4.14) that

$$\sum_{k=1}^{N}\left(\bar{g}^0_{i,\mathcal{K}^*_k,\mathcal{L}_k}-\bar{g}^0_{i,\mathcal{K}^*_{k+1},\mathcal{L}_k}\right)=0. \tag{4.23}$$

We assume that the equality (4.22) is true for some $n\geqslant 0$. Using the definition (4.16) of $\bar{g}^{n+1}_{i,\mathcal{K}^*,\mathcal{L}}$ and successively equations (4.15f)-(4.15g) then (4.15e), it follows that

$$\begin{aligned}\sum_{k=1}^{N}\left(\bar{g}^{n+1}_{i,\mathcal{K}^*_k,\mathcal{L}_k}-\bar{g}^{n+1}_{i,\mathcal{K}^*_{k+1},\mathcal{L}_k}\right)&=\sum_{k=1}^{N}\left(\psi^{n+1}_{i,\mathcal{K}^*_{k+1},\mathcal{L}_k}-\psi^{n+1}_{i,\mathcal{K}^*_k,\mathcal{L}_k}\right)+\frac{\lambda}{2}\sum_{k=1}^{N}\left(e^{n+1}_{i,\mathcal{K}^*_k}-e^{n+1}_{i,\mathcal{K}^*_{k+1}}\right)\\&=\underbrace{\sum_{k=1}^{N}\left(\bar{g}^n_{j,\mathcal{K}^*_{k+1},\mathcal{L}_k}-\bar{g}^n_{j,\mathcal{K}^*_k,\mathcal{L}_k}\right)}_{=0\text{ by induction}}+\lambda\sum_{k=1}^{N}\left(e^{n+1}_{i,\mathcal{K}^*_k}-e^{n+1}_{i,\mathcal{K}^*_{k+1}}\right)\\&=\lambda\sum_{k=1}^{N}\left(e^{n+1}_{i,\mathcal{K}^*_k}-e^{n+1}_{i,\mathcal{K}^*_{k+1}}\right)\\&=\lambda e^{n+1}_{i,\mathcal{K}^*_1}-\lambda e^{n+1}_{i,\mathcal{K}^*_{N+1}}\\&=0.\end{aligned}$$

Furthermore, we also have

$$\sum_{k=1}^{N}\left(\psi^{n+1}_{i,\mathcal{K}^*_{k+1},\mathcal{L}_k}-\psi^{n+1}_{i,\mathcal{K}^*_k,\mathcal{L}_k}\right)=\sum_{k=1}^{N}\left(\bar{g}^{n+1}_{i,\mathcal{K}^*_k,\mathcal{L}_k}-\bar{g}^{n+1}_{i,\mathcal{K}^*_{k+1},\mathcal{L}_k}\right)-\frac{\lambda}{2}\sum_{k=1}^{N}\left(e^{n+1}_{i,\mathcal{K}^*_k}-e^{n+1}_{i,\mathcal{K}^*_{k+1}}\right)=0.$$

To sum up, we proved that:

$$\left\{\begin{array}{rcl}\forall\, k\in\{1,\cdots,N\},\quad m_{\mathcal{K}^*_k,\mathcal{L}_k}\psi^{n+1}_{i,\mathcal{K}^*_k,\mathcal{L}_k}+m_{\mathcal{K}^*_{k+1},\mathcal{L}_k}\psi^{n+1}_{i,\mathcal{K}^*_{k+1},\mathcal{L}_k} & \underset{n\to+\infty}{\longrightarrow} & 0,\\ \forall\, k\in\{2,\cdots,N\},\quad m_{\mathcal{K}^*_k,\mathcal{L}_k}\psi^{n+1}_{i,\mathcal{K}^*_k,\mathcal{L}_k}+m_{\mathcal{K}^*_k,\mathcal{L}_{k-1}}\psi^{n+1}_{i,\mathcal{K}^*_k,\mathcal{L}_{k-1}} & \underset{n\to+\infty}{\longrightarrow} & 0,\\ \displaystyle\sum_{k=1}^{N}\left(\psi^{n+1}_{i,\mathcal{K}^*_{k+1},\mathcal{L}_k}-\psi^{n+1}_{i,\mathcal{K}^*_k,\mathcal{L}_k}\right) & = & 0,\end{array}\right.$$

that is to say, in a more compact form, that:

$$B\Psi^{n+1} \underset{n\to+\infty}{\longrightarrow} 0,$$

with B is the matrix being defined in (4.11). Since this matrix B is invertible, we deduce

$$\Psi^{n+1} \underset{n\to+\infty}{\longrightarrow} 0,$$

and the claim is proved.

□

5. Numerical results

We illustrate in this section the convergence properties of the Schwarz algorithm presented above on various test cases. We also illustrate how this convergence depend on λ. Finally, the performance of the method as a preconditioner is also investigated.

For each test case we give the formulas for the diffusion tensor A and the exact solution u_e from which we deduce the source term $f = -\text{div}(A\nabla u_e)$ to be used in the numerical computations.

5.1 *Initialization*

In all the following numerical simulations, we choose the initial guess for $u_i^{\mathcal{T}}$ to be

$$u_i^0 = 0, \qquad \forall\, i \in \{1,2\},$$

and we take the initial Fourier data $g_0^{\mathcal{T}_i}$ in such a way that

$$\sum_{k=1}^{N}\left(g^0_{i,\mathcal{K}_k^*,\mathcal{L}_k} - g^0_{i,\mathcal{K}_{k+1}^*,\mathcal{L}_k}\right) = \frac{\lambda}{2}\left(h_{\mathcal{K}_1^*} - h_{\mathcal{K}_{N+1}^*}\right), \qquad \forall\, i \in \{1,2\}.$$

One can take for instance, for each $i \in \{1,2\}$, $g^0_{i,\mathcal{K}_1^*,\mathcal{L}_1} = \dfrac{\lambda}{2}\left(h_{\mathcal{K}_1^*} - h_{\mathcal{K}_{N+1}^*}\right)$, and $g^0_{i,\mathcal{K}_k^*,\mathcal{L}_k} = 0$, $\forall 2 \leqslant k \leqslant N$, and $g^0_{i,\mathcal{K}_{k+1}^*,\mathcal{L}_k} = 0$, $\forall 1 \leqslant k \leqslant N$.

Following Theorem 4.2, this choice will imply the convergence of the flux unknowns $\varphi^n_{i,\mathcal{K}^*,\mathcal{L}}$.

5.2 *The domains and the meshes*

In the sequel, Ω will be a domain decomposed into rectangular subdomains $\Omega = \bigcup\limits_{k=1}^{N} \Omega_k$, with N equal to $2, 3$ or 4.

Figures 5.1, 5.2, 5.3, 5.4 and 5.5 show the coarsest meshes Mesh_1^k of the family of refined meshes $(\text{Mesh}_m^k)_m$ that we use in the sequel. More precisely, Mesh_m^k is obtained from Mesh_{m-1}^k by dividing into two equal parts all the edges in the mesh, which implies that each control volume is divided into four parts.

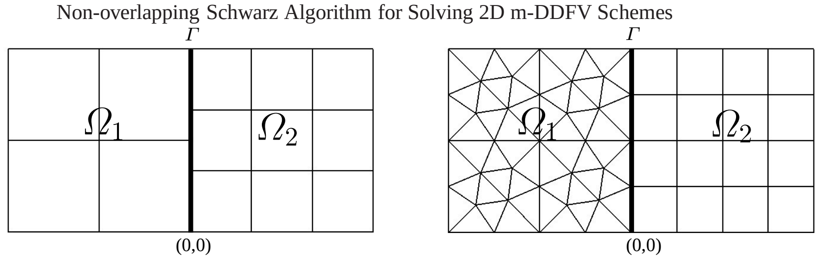

FIG. 5.1. The domain $\Omega = [-1, 1] \times [0, 1]$ is divided in 2 subdomains. (Left) Mesh_1^1. (Right) Mesh_1^2.

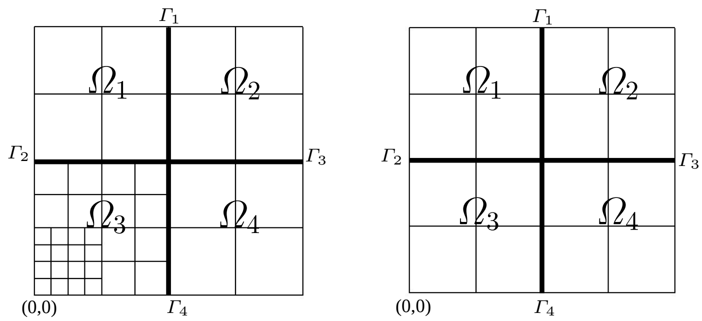

FIG. 5.2. The domain $\Omega = [0, 1]^2$ is divided in 4 subdomains. (Left) Mesh_1^3. (Right) Mesh_1^4.

5.3 *Convergence of the Schwarz algorithm used as a solver*

Let us first illustrate the convergence of the Schwarz algorithm on some simple cases.

- Case 1 : Homogeneous Dirichlet Boundary Conditions:

$$u_e(x, y) = \sin(\pi x) \sin(\pi y) \sin(\pi(x + y)),$$

  and

$$A(x, y) = \begin{pmatrix} 1.5 & 0.5 \\ 0.5 & 1.5 \end{pmatrix} \text{ for } x < 0, \quad \text{and } A(x, y) = \begin{pmatrix} 1.5 & 0.5 \\ 0.5 & 1 \end{pmatrix} \text{ for } x > 0.$$

- Case 2 : Non Homogeneous Dirichlet Boundary Conditions:

$$u_e(x, y) = \cos(2.5\pi x) \cos(2.5\pi y),$$

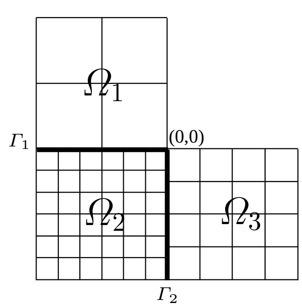

FIG. 5.3. The L-shaped domain $\Omega = [-0.5, 0.5]^2 \backslash [0, 0.5]^2$ is divided in 3 subdomains. Mesh_1^5.

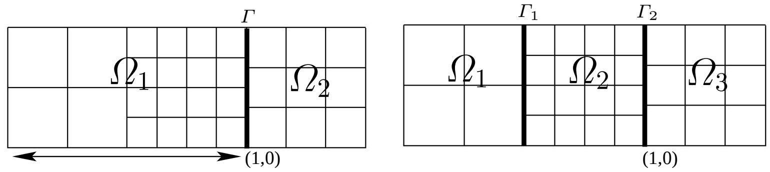

FIG. 5.4. The domain $\Omega = [-1,2] \times [0,1]$. (Left) Ω is divided in 2 subdomains Mesh_1^6. (Right) Ω is divided in 3 subdomains Mesh_1^7.

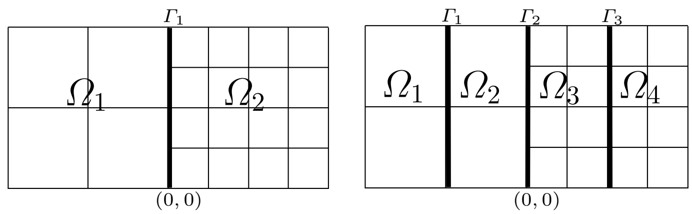

FIG. 5.5. The domain $\Omega = [-1,1] \times [0,1]$. (Left) Ω is divided in 2 subdomains Mesh_1^8. (Right) Ω is divided in 4 subdomains Mesh_1^9.

and

$$A(x,y) = \begin{pmatrix} 1.5 & 0.5 \\ 0.5 & 1.5 \end{pmatrix} \text{ for } x < 0, \quad \text{ and } A(x,y) = \begin{pmatrix} 1.5 & 0.5 \\ 0.5 & 1 \end{pmatrix} \text{ for } x > 0.$$

In order to illustrate the convergence of the Schwarz algorithm, we decide to stop the algorithm when

$$\frac{||u_n^{\mathcal{T}_i} - u^{\mathcal{T}_i}||_2}{||u^{\mathcal{T}_i}||_2} < 10^{-7}.$$

We observe for Case 1 (resp. Case 2) on meshes Mesh_5^1 and Mesh_5^2, (see Figure 5.6), that almost 10^3 iterations are necessary to achieve convergence.

Since $u_n^{\mathcal{T}_i}$ converges to $u^{\mathcal{T}_i}$ when n goes to ∞, for $i = 1, 2$, we expect the error $\frac{||u_n^{\mathcal{T}_i} - u_e||_2}{||u_e||_2}$ to be of the same order than $\frac{||u^{\mathcal{T}_i} - u_e||_2}{||u_e||_2}$, for large enough values of n. Thus, a natural stopping criterion could be the following

$$\frac{||u_n^{\mathcal{T}_i} - u^{\mathcal{T}_i}||_2}{||u^{\mathcal{T}_i}||_2} < \eta \frac{||u^{\mathcal{T}_i} - u_e||_2}{||u_e||_2}, \tag{5.1}$$

for some $\eta < 1$. Unfortunately, in practical cases u_e is obviously *a priori* unknown, but we know that the error for the m-DDFV scheme behaves like h^α where $\alpha = 1$ in general and $\alpha = 2$ for rectangular meshes. Hence, we can use, in practice, the following stopping criterion

$$\frac{||u_n^{\mathcal{T}_i} - u^{\mathcal{T}_i}||_2}{||u^{\mathcal{T}_i}||_2} < \eta h^\alpha, \tag{5.2}$$

with $\eta = 0.1$.

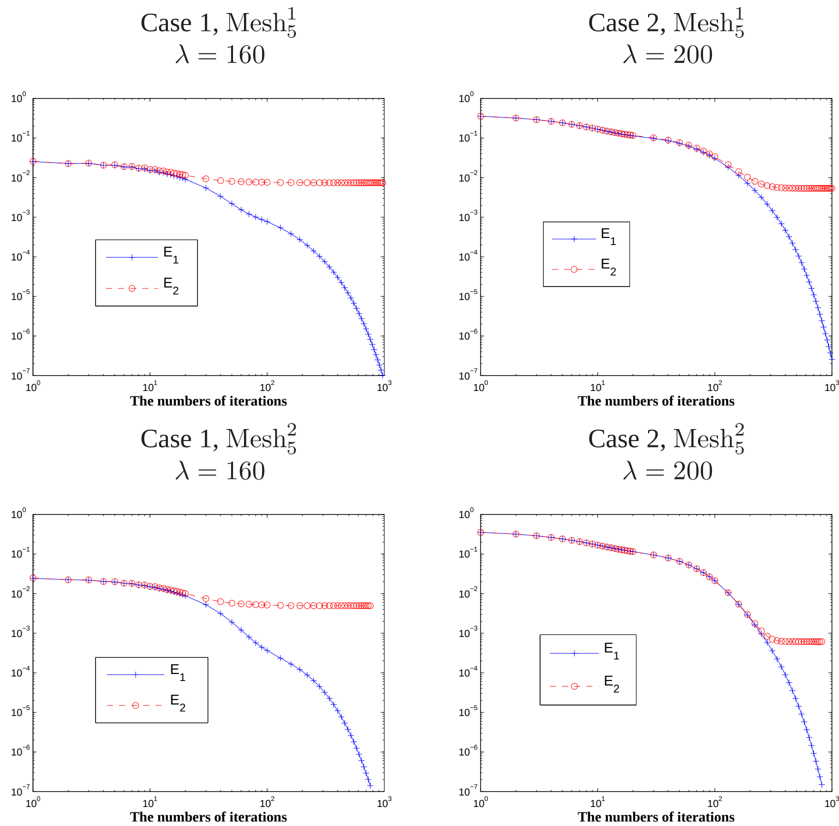

FIG. 5.6. Evolution of $E_1 = \dfrac{||u_n^{\mathcal{T}_i} - u^{\mathcal{T}_i}||_2}{||u^{\mathcal{T}_i}||_2}$ and $E_2 = \dfrac{||u_n^{\mathcal{T}_i} - u_e||_2}{||u_e||_2}$ as a function of the number of iterations. (Left) Case 1. (Right) Case 2.

Let us investigate the number of iterations required to achieve condition (5.1) in the following cases proposed in the *Benchmark on Discretization Schemes for Anisotropic Diffusion Problems on General Grids* elaborated for the FVCA5 conference [11].

- Case 3 : Mild anisotropy diffusion:

$$u_e(x,y) = \sin((1-x)(1-y)) + (1-x)^3(1-y)^2, \qquad A = \begin{pmatrix} 1.5 & 0.5 \\ 0.5 & 1.5 \end{pmatrix}.$$

- Case 4 : Heterogeneous rotating anisotropy diffusion:

$$u_e(x,y) = \sin(\pi x)\sin(\pi y), \qquad A(x,y) = \frac{1}{x^2+y^2}\begin{pmatrix} 10^{-3}x^2 + y^2 & (10^{-3}-1)xy \\ (10^{-3}-1)xy & x^2 + 10^{-3}y^2 \end{pmatrix}.$$

Table 1 gives the iteration number nbit needed to fulfill (5.1).

Case 3 - Mesh_5^3 - $\lambda = 160$	$\mathrm{nbit} = 99$
Case 4 - Mesh_5^4 - $\lambda = 205$	$\mathrm{nbit} = 134$

Table 1. Iteration number nbit needed to fulfill (5.1) for cases 3 and 4.

Case 5 illustrates the behaviour of the Schwarz algorithm when $u_e \notin H^2(\Omega)$. The first order error estimate for m-DDFV given in Theorem 3.1 is no more valid. Nevertheless, the scheme is known to be convergent (see [2]).

- Case 5 : Isotropic constant diffusion on an L-shaped domain, $u_e \notin H^2(\Omega)$:

$$u_e(x,y) = u_e(r,\theta) = r^{\frac{2}{3}} \sin\left(\frac{2}{3}\left(\theta + \frac{\pi}{2}\right)\right), \qquad A = \begin{pmatrix} 1 & 0 \\ 0 & 1 \end{pmatrix}.$$

Table 2 gives the iteration number nbit needed to fulfill (5.1).

Case 5 - Mesh_5^5 - $\lambda = 800$	$\mathrm{nbit} = 139$

Table 2. Iteration number nbit needed to fulfill (5.1) for Case 5.

5.4 *Influence of the shape of the domain decomposition*

We compare the algorithm for different decompositions of the same domain $\Omega = [-1,2] \times [0,1]$ (see Figure 5.4) and for the same test case corresponding to a spatially localized source term.

- Case 6 : Anisotropic diffusion. The source term is given by

$$f(x,y) = \begin{cases} -1000 \sin(2.5\pi(x-1.3)) & \text{for } 1.3 < x < 1.7, \\ 0 & \text{otherwise,} \end{cases}$$

  and the diffusion tensor by

$$A(x,y) = \begin{pmatrix} 1.5 & 0.5 \\ 0.5 & 1.5 \end{pmatrix} \text{ for } x < 0 \text{ or } x > 1, \qquad \text{and } A(x,y) = \begin{pmatrix} 1.5 & 0.5 \\ 0.5 & 1 \end{pmatrix} \text{ otherwise.}$$

  The exact solution is given by

$$u_e(x,y) = \begin{cases} x & \text{for } -1 < x < 1.3, \\ x + \dfrac{1000}{1.5}\left(\dfrac{x-1.3}{2.5\pi} - \dfrac{1}{(2.5\pi)^2}\sin(2.5\pi(x-1.3))\right) & \text{for } 1.3 < x < 1.7, \\ x + \dfrac{1000}{1.5}\left(\dfrac{1}{5\pi} - \dfrac{1}{(2.5\pi)^2}\sin(5\pi)\right) & \text{for } 1.7 < x < 2. \end{cases}$$

Figure 5.7 is representing the error $|u_{11}^{\mathcal{T}} - u^{\mathcal{T}}|$ on the primal mesh (resp. dual mesh) with $\lambda = 250$.

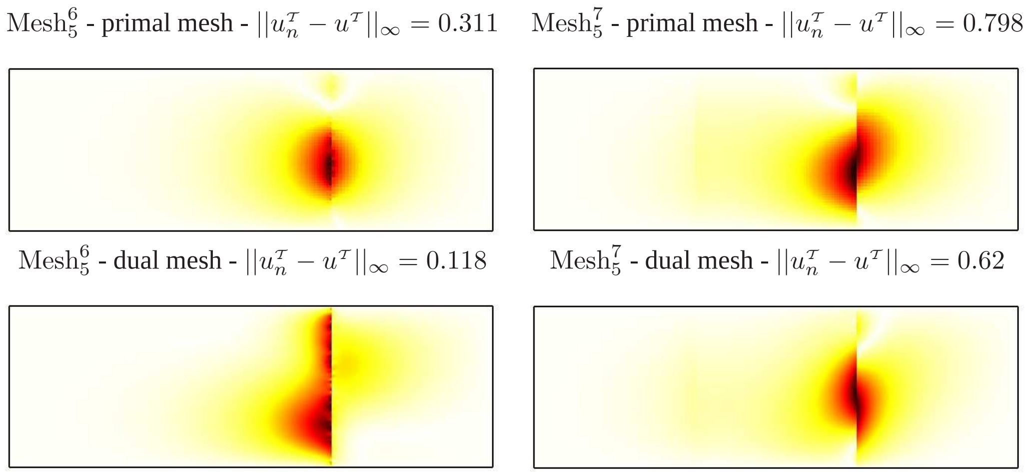

FIG. 5.7. Plot of $|u_n^{\mathcal{T}} - u^{\mathcal{T}}|$. Case 6, $\lambda = 250$, iteration $n = 11$. (Left) two domains decomposition $\Omega = \Omega_1 \cup \Omega_2$. (Right) three domains decomposition $\Omega = \Omega_1 \cup \Omega_2 \cup \Omega_3$.

The supremum norm $||u_n^{\mathcal{T}} - u^{\mathcal{T}}||_\infty$ for the decomposition into 2 subdomains (Mesh_5^6) on the primal (resp. dual) mesh decreases from 1.07 (resp. 0.4) to 0.31 (resp. 0.12) after 10 iterations. For the decomposition into 3 subdomains (Mesh_5^7) $||u_n^{\mathcal{T}} - u^{\mathcal{T}}||_\infty$ on the primal (resp. dual) mesh decreases from 1.1 (resp. 1.08) to 0.8 (resp. 0.62) after 10 iterations. Notice that the composite mesh $\mathcal{T}$ is the same for the two decompositions under study. It seems that, for this localized source term, the decomposition into 2 subdomains is more accurate.

5.5 *Influence of the Fourier parameter λ*

Until now, the value of $\lambda > 0$ was arbitrarily fixed, but it is known that the choice of λ generally influences the number of necessary iterations needed to achieve convergence of the algorithm (see [1]). We illustrate this behavior in our framework in Figure 5.8. The optimal choice for λ, as shown in Figure 5.8, seems to increase with the number of degrees of freedom.

More precisely, we give in Table 3 the optimal value of λ as a function of the mesh size for the Case 2. Since the mesh size h is divided by 2 at each level of refinement, we observe that, in that case, λ_{opt} seems to behave like $\frac{1}{h}$ as described in [7], [8].

	Mesh_3^2	Mesh_4^2	Mesh_5^2
λ_{opt}	94	164	333

Table 3. The optimal value of λ as a function of the size of the mesh h for the Case 2

Let us consider again the case 6 with 2 different decompositions of Ω with the stopping criterion parameter $\eta = 0.01$. For our particular source term, we see in Figure 5.9 that for the decomposition into 2 subdomains we need less than 20 iterations to achieve (5.1) for any λ, $0.1 \leqslant \lambda \leqslant 400$, whereas for the decomposition into 3 subdomains we need at least 60 iterations (achieved around $\lambda \sim 225$). Table

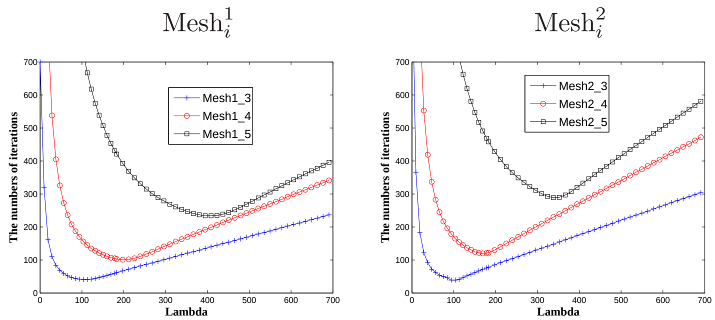

FIG. 5.8. The number of necessary iterations as a function of the λ value for Case 2.

4 sums up the iteration number nbit needed to achieve (5.1) with $\eta = 0.01$ for the optimal value of λ. Hence, in that case the decomposition into 2 subdomains is more efficient than the decomposition into 3 subdomains, which is quite natural.

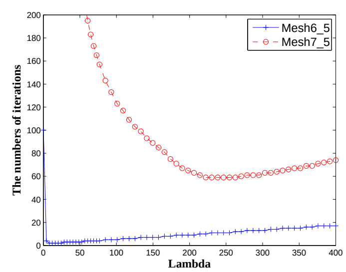

FIG. 5.9. Case 6 - The number of necessary iterations as a function of λ for the two meshes mesh_5^6 and mesh_5^7

2 subdomains $\lambda_{opt} = 20$	$\mathrm{nbit} = 2$
3 subdomains $\lambda_{opt} = 250$	$\mathrm{nbit} = 59$

Table 4. Iteration number nbit needed to fulfill (5.1) for Case 6.

In fact, this behavior is not always observed, and we will now give an example where increasing the number of subdomains in the decomposition of Ω actually improves the performance of the solver. Let us consider again the test case 1 with 2 different decompositions of Ω into 2 or 4 subdomains that is with the meshes Mesh_j^8 and Mesh_j^9 (see Figure 5.5) for different levels of refinement ($j = 3$ or $j = 5$). For the coarsest meshes ($j = 3$), left-hand side part of Figure 5.10 shows that the performance of the solver for the two decompositions are equivalent. Nevertheless, for finer meshes ($j = 5$), the right-hand part of the same figure shows that for the decomposition into 4 subdomains we need less than 36 iterations to achieve (5.1) for any $10 \leqslant \lambda \leqslant 300$, whereas for the decomposition into 2 subdomains we need at least 135 iterations (achieved around $\lambda \sim 150$).

As a conclusion, for this test case larger is the number of subdomains better seems to be the performance of the solver.

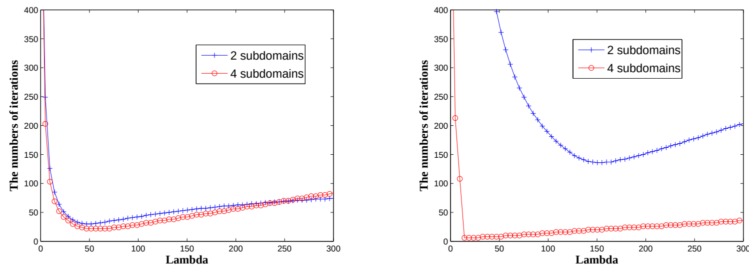

FIG. 5.10. Case 1 - The number of necessary iterations as a function of λ for the two mesh families mesh_j^8 and mesh_j^9. (Left) For $j = 3$. (Right) For $j = 5$.

5.6 *Application to the preconditioning of the conjugate gradient solver*

The non-overlapping Schwarz method we study in this paper is primarily an iterative solver for our finite volume scheme. Nevertheless, we saw in previous sections that its performances can be poor, at least if we do not choose the optimal value of the Fourier parameter associated to a given situation (it depends on the anisotropy and heterogeneity of the problem, but also on the mesh itself and the subdomains considered). Since the value of this optimal parameter is not always known precisely, we can also take advantage of the domain decomposition method by considering it as a preconditioner.

Indeed, both efficiency and robustness of iterative techniques can be improved by using preconditioning. It simply consists in solving a linear system that admits the same solution as the original one. In order to speed up iterative methods, this new linear system is chosen to have a better conditioning property. We refer to the standard preconditioning techniques in [14]. In particular, the non overlapping Schwarz methods can be seen as block Jacobi solvers, and then we know that a few iterations of the domain decomposition algorithm can be an efficient preconditioner for the conjugate gradient method.

We propose in this section some illustrations by evaluating the number of iterations necessary to achieve convergence of the conjugate gradient method. We study in particular how it depends on the number n of Schwarz subiterations we used as a preconditioner at each main iteration of the CG. A number of subiterations $n = 0$ means that no preconditioning was used. The test case we used is described below and the results are given in Figure 5.11.

- Case 7 : Constant anisotropic diffusion:

$$u_e(x, y) = 16y(1 - y)(1 - x^2), \text{ and } A(x, y) = \mathrm{Id}.$$

We observe that for reasonable values of n (here, $n = 3$), the number of necessary CG iterations increases very slowly with respect to the size of the linear system we are solving. Hence, our Schwarz method seems to be a satisfactory preconditioner for solving the m-DDFV numerical scheme.

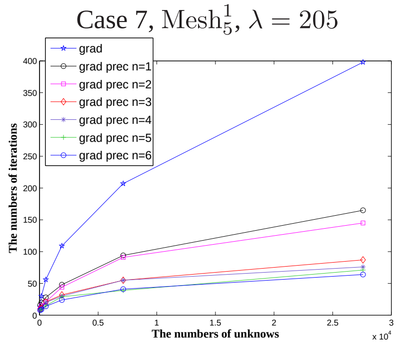

FIG. 5.11. The number of iterations as a function of the number of unknowns.

As shown in Section 5.5, the value of the Fourier parameter λ has an influence on the performance of the Schwarz algorithm and it seems that there exists an optimal choice for this value. We want to see now if there exists also an optimal choice of the value of λ when the Schwarz method is used as preconditioner. To this end, we consider the results obtained for the test case 7. The optimal value of λ for the Schwarz algorithm, used as an iterative solver, is around 115 (see Figure 12(a)) to achieve an error of 10^{-8}. Figure 12(b) is also showing the number of iterations of the conjugate gradient solver preconditioned by 2 subiterations of the Schwarz algorithm necessary to achieve the same precision as a function of λ. We observe that the influence of λ is not so clear than for the Schwarz algorithm as a solver but it seems that the optimal value of λ is around 3 (see the zoom in Figure 12(c)).

6. Conclusions

In this paper, we proposed a m-DDFV finite volume scheme with mixed Dirichlet/Fourier boundary conditions for anisotropic elliptic problems. As a result, we provide a non-overlapping Schwarz algorithm associated to a subdomain decomposition of Ω for solving the m-DDFV scheme. The Schwarz algorithm we obtained is proved to converge to the solution of the m-DDFV scheme on the whole domain. The properties of this algorithm are illustrated by numerical results on anisotropic elliptic equations. We illustrate in particular the existence of a unique value of the Fourier parameter for which the convergence is the fastest. Nevertheless, we also observe that, as usual, the performances of such a method as a solver are not very good whereas it is of real practical interest to use a few sub-iterations of this algorithm as a preconditioner for the conjugate gradient solver.

In further works, such a Fourier/Robin transmission condition should be compared to second order optimized condition or to two-sided Robin condition in this DDFV framework as it is done in [10] for the classical two point flux approximation finite volume approach.

Acknowledgments : The authors would like to thank the referees for their careful reading of the paper and their valuable remarks.

REFERENCES

[1] Y. Achdou, C. Japhet, Y. Maday, and F. Nataf. A new cement to glue non-conforming grids with robin interface

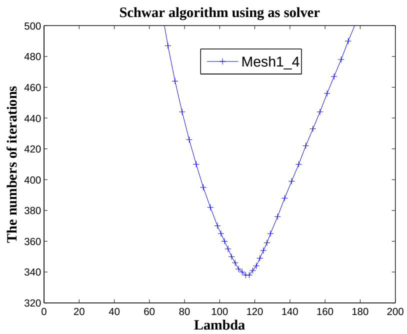

(a) Schwarz algorithm.

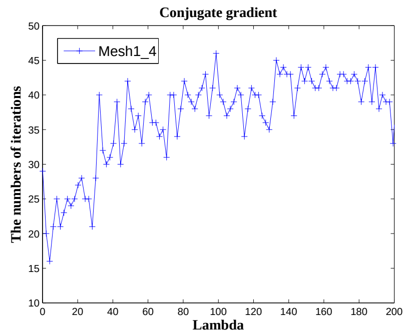

(b) Conjugate gradient method.

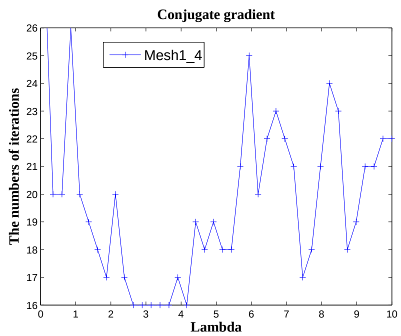

(c) Zoom $\lambda \in [0, 10]$.

FIG. 5.12. The number of iterations to achieve an error of 10^{-8} as a function of λ. Case 7.

conditions: The finite volume case. *Numer. Math.*, 92(4):593–620, 2002.

[2] B. Andreianov, F. Boyer, and F. Hubert. Discrete duality finite volume schemes for Leray-Lions type elliptic problems on general 2D-meshes. *Num. Meth. for PDEs*, 23(1):145–195, 2007.

[3] F. Boyer and F. Hubert. Finite volume method for 2d linear and nonlinear elliptic problems with discontinuities. *SIAM J. Numer. Anal.*, to appear, 2008.

[4] R. Cautrès, R. Herbin, and F. Hubert. The Lions domain decomposition algorithm on non-matching cell-centred finite volume meshes. *IMA J. Numer. Anal.*, 24(3):465–490, 2004.

[5] S. Delcourte, K. Domelevo, and P. Omnes. A discrete duality finite volume approach to Hodge decomposition and div-curl problems on almost arbitrary two-dimensional meshes. *SIAM J. Numer. Anal.*, 45(3):1142–1174 (electronic), 2007.

[6] K. Domelevo and P. Omnes. A finite volume method for the Laplace equation on almost arbitrary two-dimensional grids. *M2AN Math. Model. Numer. Anal.*, 39(6):1203–1249, 2005.

[7] O. Dubois. *Optimized Schwarz Methods for the Advection-Diffusion Equation and for Problems with Discontinuous Coefficients*. PhD thesis, McGill University in Montréal, Canada, June 2007.

[8] M. J. Gander. Optimized Schwarz method. *SIAM Journal on Numerical Analysis*, 44(2):699–731, 2006.

[9] M. J. Gander, C. Japhet, Y. Maday, and F. Nataf. A new cement to glue nonconforming grids with Robin interface conditions: the finite element case. *Lect. Notes Comput. Sci. Eng.*, 40:259–266, 2005.

[10] L. Halpern and F. Hubert. Optimized schwarz algorithms in the classical finite volume framework. *in preparation*, 2008.

[11] R. Herbin and F. Hubert. Benchmark on discretization schemes for anisotropic diffusion problems on general grids. In R. Eymard and J. M. Herard, editors, *Proceedings of Finite Volumes for Complex Applications V*. Hermès, 2008.

[12] F. Hermeline. Approximation of diffusion operators with discontinuous tensor coefficients on distorted meshes. *Comput. Methods Appl. Mech. Engrg.*, 192(16-18):1939–1959, 2003.

[13] P.-L. Lions. On the Schwarz alternating method. III. A variant for nonoverlapping subdomains. In *Third International Symposium on Domain Decomposition Methods for Partial Differential Equations (Houston, TX, 1989)*, pages 202–223. SIAM, Philadelphia, PA, 1990.

[14] Y. Saad. *Iterative methods for sparse linear systems*. Society for Industrial and Applied Mathematics, Philadelphia, PA, second edition, 2003.